MICROCOPY RESOLUTION TEST CHART

NATIONAL BUREAU OF STANDARDS-1963-A

LEVEL

AIR FORCE INSTITUTE OF TECHNOLOGY

AIR UNIVERSITY
UNITED STATES AIR FORCE

D D

FEB 21

A

# SCHOOL OF ENGINEERING

WRIGHT-PATTERSON AIR FORCE BASE, OHIO

MODEM MODELING AND
CHARACTERIZATION

THESIS

AFIT/GE/EE/78-30   ROBERT L. JONES
Captain   USAF
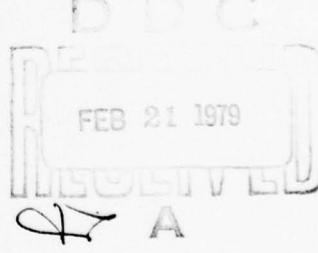
Approved for public release; distribution unlimited

19 Jan 79

JOSEPH P. HIPPS, Major, USAF
Director of Information

AFIT/GE/EE/78-30

MODEM MODELING AND CHARACTERIZATION.

THESIS Master's thesis,

Presented to the Faculty of the School of Engineering

of the Air Force Institute of Technology

Air University

in Partial Fulfillment of the

Requirements for the Degree of

Master of Science

105 P'

by

Robert L. Jones, B.S.E.E.

Captain   USAF

Graduate Electrical Engineering

December 1978

Approved for public release; distribution unlimited

Preface

The objective of this thesis was to develop a method to
identify the type of modulator-demodulator (modem) used on
various communications links for the Automated Tech Control
(ATEC). I chose to model and characterize seven modems,
choosing as the characterization the power spectral density
and autocorrelation function of the output signal from each
of the seven modems. I also used the equations for the
power spectral density of five of the modems to determine
the data rate at which these modems were operating.

I would like to express my appreciation and acknowledge
my indebtedness to Major Joseph W. Carl, Assistant Professor
in the AFIT Electrical Engineering Department and thesis
advisor for his advice and guidance during this investiga-
tion.

And last but not least, a debt of gratitude is due my
wife and son. May we once again renew our acquaintances.

Robert L. Jones

Contents

Contents

List of Figures

List of Figures

List of Tables

AFIT/GE/EE/78-30

Abstract

A method for modem modeling and characterization is presented. The properties of Fourier transforms and the properties of correlation and power spectral density for periodic and random functions are reviewed. The modems modeled are characterized by the theoretical calculation of the power spectral density and autocorrelation function of the output signal from the modem under ideal conditions. The input signal to the modems characterized is either a random pulse train or a special periodic function. Also, power spectral density curves are constructed to determine the data rate at which a modem is operating. Though no empirical data exists, the theoretical calculations indicate that modems can be characterized by the power spectral density and the autocorrelation function. More research, however, is needed for accurately determining the data rate at which a modem is operating.

MODEM MODELING AND CHARACTERIZATION

I. Introduction

As more and more sophisticated communications systems
are developed, one basic goal still remains the same: the
receiver must produce as its output a recognizable replica
of the information that is transmitted to it from a source
through some type of medium commonly called a channel. A
typical system diagram appears in Figure 1.
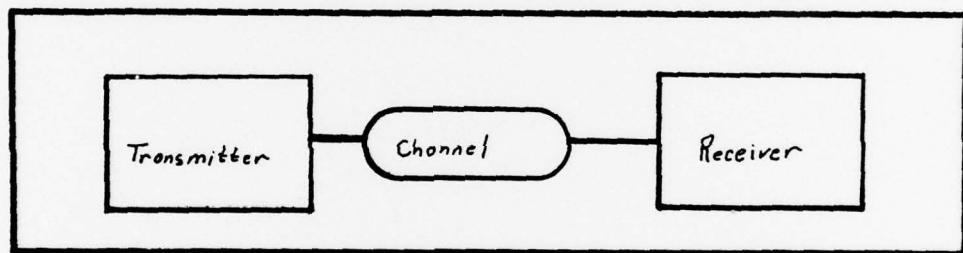
Figure 1. Block Diagram of a Basic Communications
System (Ref 9:2)

Because the information being transmitted usually
occupies baseband frequencies near dc, it is usually neces-
sary to shift the baseband channel to a more appropriate
location in the frequency spectrum for transmission. In
most communications work, information transmission is close-
ly related to the modulation or time variation of a par-
ticular sinusoidal signal, called the carrier, by a device
called a modulator. In order to obtain the information

1

from the carrier, the received signal must be demodulated by a similar device operating as the inverse of the modulator. Devices used for modulation and demodulation are commonly called MODEMS. A typical system diagram is shown in Figure 2, where $\underline{x}_b(t)$ is the baseband signal, $\underline{x}_p(t)$ is the modulated signal, $\underline{y}_p(t)$ is the modulated signal received after transmission over the channel, and $\underline{y}_b(t)$ is the demodulated signal or a replica of $\underline{x}_b(t)$, the original message signal. The modulated signal, $\underline{y}_p(t) = \underline{x}_p(t) + \underline{n}(t)$ where $\underline{n}(t)$ is noise added to $\underline{x}_p(t)$ by the channel.
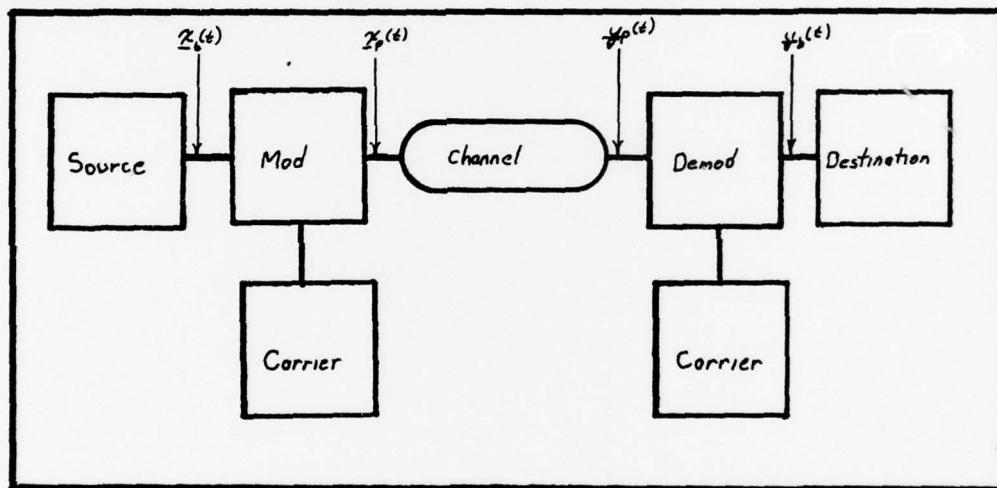
Figure 2. Block Diagram of Carrier System for Signal Transmission (Ref 2:119)

Problem and Scope

The Air Force Communications Service (AFCS) in conjunction with the Rome Air Development Center (RADC) is engaged in research in the area of modem identification for the Automated Tech Control (ATEC) and the possible use of degradation analysis of communications links based on the type of

2

modem connected to the links.

The goal of this thesis is to develop a method to identify the type of modem used on a communications link based on real time measurement of $y_p(t)$ or $y_b(t)$ (Figure 2). The identification consists of determining the modulation scheme and the data rate at which the modem is operating. This study is intended to support the report (Ref 1) prepared by AFSC/OA, although a theoretical rather than a trial and error approach is taken.

There are three basic ways of modulating a sinusoidal carrier: variation of its amplitude, phase, and frequency in accordance with the information being transmitted. Other modulation schemes are just variations and/or combinations of one or more of the basic modulation schemes. In this study, seven different modulation schemes or modems are mathematically modeled and characterized for identification. They are:

1. Binary Phase Shift Keying (BPSK)
2. Quadrature Phase Shift Keying (QPSK)
3. Binary Frequency Shift Keying (BFSK)
4. Duobinary Frequency Shift Keying (DBFSK)
5. Binary Amplitude Shift Keying (BASK)
6. Double Sideband Amplitude Modulation (DSBAM)
7. Double Sideband Amplitude Modulation with Suppressed Carrier (DSBAM-SC)

The input signal used with the first five modulation schemes is a random pulse train with a basic pulse P(t)

having magnitude 1 and signaling interval T as shown in Figure 3, while the input used with the last two modulation schemes is the special periodic function, $\gamma \cos w_s t$.
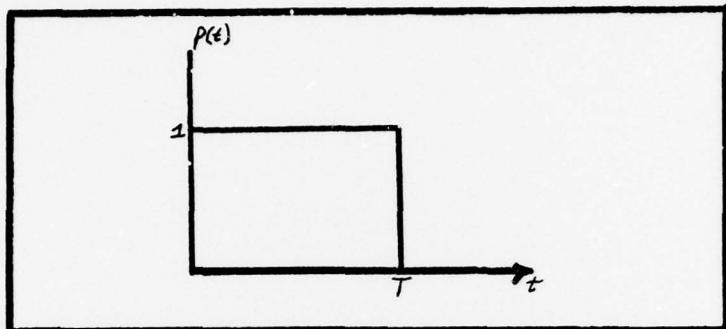
Figure 3. Basic Pulse Shape
of Binary Input Signal

The modems are modeled in the absence of noise (i.e., $\underline{n}(t) = 0$) using the following assumptions:

1. The channel is ideal and introduces no anomalies in the transmitted signal (i.e., $\underline{x}_p(t) = \underline{y}_p(t)$).

2. The transmitter is ideal and introduces no anomalies in the transmitted signal.

3. The input signal is a random pulse train represented as $\underline{x}_b(t) = \sum\limits_{n=o}^{+\infty} \underline{b}_n P(t - nT)$ where the $\underline{b}_n$'s are identically independently distributed Bernoulli random variables each equally likely to be zero or one and where the values of $\underline{b}_n$ are independent of each other.

4. The negative frequency terms do not overlap the positive frequency terms (i.e., $X(w - w_c)$ does not overlap $X(w + w_c)$).

4

The modems are characterized by the power spectral density and the correlation function of the modulated signal $\underline{x}_p(t)$ shown in Figure 2 since the channel was assumed ideal (i.e., $\underline{y}_p(t) = \underline{x}_p(t)$ and $\underline{y}_b(t) = \underline{x}_b(t)$).

Approach and Outline

First, the theory and properties of Fourier transforms, correlation, and power spectral density are presented in Chapter II. Next, the method used in modeling the modems as well as a general operational description is presented in Chapter III. The procedures used in characterizing the modems is presented in Chapter IV. Discussion of the results from the study are covered in Chapter V and the conclusions and recommendations are presented in Chapter VI.

Conventions

The following conventions are used:

1. The underlining of a variable indicates that it is a random variable (e.g., $\underline{x}$).

2. The underlining of an explicit function of time indicates that it is a random process (e.g., $\underline{x}(t)$).

3. The use of the asterisk (*) as a superscript indicates complex conjugate (i.e., $X^*(w)$ is the complex conjugate of $X(w)$).

II.   Fourier Transforms, Correlation, and Power Spectral Density

Introduction

The Fourier transform, correlation, and power spectral density find many applications in engineering and the purpose of this section is to acquaint the reader with some of the properties of each of these used in this study.

Fourier Transforms

There exists a variety of notation to denote the Fourier transform pair, but the following notation and transform pair will be used in this study. Eq (1) is the Fourier transform of x(t), which in general is a complex-domain to complex-domain transformation; whereas Eq (2) is the inverse Fourier transform of X(w), which in general is a complex-domain to complex-domain transformation.

$$X(w) = F\left[x(t)\right]$$

$$X(w) = \int_{-\infty}^{+\infty} x(t)e^{-jwt}dt \tag{1}$$

$$x(t) = \frac{1}{2\pi} \int_{-\infty}^{+\infty} X(w)e^{jwt}dw \tag{2}$$

This transform pair exists and is unique provided that the function x(t) satisfies the following:

1. $\int_{-\infty}^{+\infty} |x(t)|\ dt < +\infty$

2.   Any discontinuities in x(t) are finite (Ref 4:9).

6

Some Properties of One-Dimensional Fourier Transforms

Symmetry. Magnitude and the real part of the Fourier transform are even functions, while phase and the imaginary portion of the Fourier transform are odd valued functions. This is easily seen if Euler's identity for e^{-jwt} is used, then Eq (1) can be expressed as

$$X(w) = \int_{-\infty}^{+\infty} x(t) \, (\cos wt - j \sin wt) \, dt \qquad (3)$$

where $e^{-jwt} = \cos wt - j \sin wt$.

Now the real part of Eq (3) is

$$Re \, [X(w)] = \int_{-\infty}^{+\infty} x(t) \cos wt \, dt \qquad (4)$$

while the imaginary part of Eq (3) is

$$Im \, [X(w)] = \int_{-\infty}^{+\infty} x(t) \sin wt \, dt \qquad (5)$$

Because cosine is an even function and sine is an odd function, it follows that

$$Re \, [X(w)] = Re \, [X(-w)] \qquad (6)$$

$$Im \, [X(w)] = -Im \, [X(-w)] \qquad (7)$$

Since the transform is in general a complex number, the magnitude of the transform is even valued and is given by

$$|X(w)| = \sqrt{\{Re \, [X(w)]\}^2 + \{Im \, [X(w)]\}^2} \qquad (8)$$

The phase of the transform is expressed by

$$\Phi(w) = \tan^{-1}\left\{ \operatorname{Im}\left[X(w)\right] / \operatorname{Re}\left[X(w)\right]\right\} \tag{9}$$

and is, therefore, odd valued since the imaginary part of the transform is odd.

Linearity. The Fourier transform of a transformable function is a linear transformation, which follows directly from the additive property of integration. Let $x(t) = \alpha h_1(t) + \beta h_2(t)$, where α and β are constants. Then the Fourier transform of $x(t)$ using Eq (1) is

$$F\left[x(t)\right] = \int_{-\infty}^{+\infty} \left[\alpha h_1(t) + \beta h_2(t)\right] e^{-jwt} dt$$

$$= \alpha \int_{-\infty}^{+\infty} h_1(t) e^{-jwt} dt + \beta \int_{-\infty}^{+\infty} h_2(t) e^{-jwt} dt$$

$$= \alpha X_1(w) + \beta X_2(w) \tag{10}$$

where $X_1(w)$ is the transform of $h_1(t)$ and $X_2(w)$ is the transform of $h_2(t)$.

Time Shifted. What happens to the transform of a function which has been shifted in time? Let $x(t) = g(t - T)$, then the transform is

$$F\left[x(t)\right] = \int_{-\infty}^{+\infty} g(t - T) e^{-jwt} dt \tag{11}$$

This equation can be reduced by using the change of variable $u = t - T$. Then Eq (11) becomes

8

$$F\left[x(t)\right] = \int_{-\infty}^{+\infty} g(u)e^{-jw(u+T)}du$$

$$= e^{-jwT} \int_{-\infty}^{+\infty} g(u)e^{-jwu}du$$

$$= e^{-jwT}G(w) \tag{12}$$

Where $G(w)$ is the Fourier transform of $g(t)$ by using Eq (1).
In other words, the transform of a function which has been
shifted by an amount T is just the transform of the original
function multiplied by e^{-jwT}.

Modulation. What happens to the transform of a func-
tion which is being modulated by a cosinusoidal signal?
Let $x(t)$ be modulated by $\cos w_c t$, then the transform is

$$F\left[x(t)\cos w_c t\right] = \int_{-\infty}^{+\infty} x(t)\cos w_c t e^{-jwt}dt \tag{13}$$

This equation can be reduced by using Euler's identity for
$\cos w_c t = (e^{+jw}c + e^{-jw}c) / 2$. Then Eq (13) becomes

$$F\left[x(t)\cos w_c t\right] = \int_{-\infty}^{+\infty} x(t)e^{jw_c t}e^{-jwt}dt$$

$$+ \int_{-\infty}^{+\infty} x(t)e^{-jw_c t}e^{-jwt}dt$$

$$= 1/2 \int_{-\infty}^{+\infty} x(t)e^{-jt(w-w_c)}dt$$

$$+ 1/2 \int_{-\infty}^{+\infty} x(t)e^{-jt(w+w_c)}dt \tag{14}$$

9

and using the form of Eq (1) where $w = w - w_c$ and $w + w_c$, then

$$F\left[x(t)\cos w_c t\right] = 1/2X(w + w_c) + 1/2X(w - w_c) \quad (15)$$

Frequency Translation. What happens to the transform of a function which has been frequency translated? Let $z(t) = x(t)e^{jw_c t}$, then the transform is

$$F\left[x(t)e^{jw_c t}\right] = \int_{-\infty}^{+\infty} x(t)e^{jw_c t}e^{-jwt}dt$$

$$= \int_{-\infty}^{+\infty} x(t)e^{-jt(w-w_c)}dt \quad (16)$$

and using the form of Eq (1) where $w = w - w_c$, then

$$F\left[x(t)e^{jw_c t}\right] = X(w - w_c) \quad (17)$$

Multiplication. What happens to the transform of two functions that are multiplied together? Let $x(t) = x_1(t)x_2(t)$, then the transform is

$$F\left[x_1(t)x_2(t)\right] = \int_{-\infty}^{+\infty} x_1(t)x_2(t)e^{-jwt}dt \quad (18)$$

Using Eq (17) the result is

$$F\left[x_1(t)x_2(t)\right] = \int_{-\infty}^{+\infty} X_1(w - w_c)X_2(w_c)dw \quad (19)$$

where $X_1(w - w_c)$ is the transform of $x_1(t)e^{-jwt}$ and

$X_2(w_c)$ is the transform of $X_2(t)$.

Correlation Function

Definition. If there exists a system with an input x and an output y, it is possible to write a statistical relationship such as $f(x,y)$, the joint density function between x and y. If there are no disturbing influences in the system, then x and y will be uniquely related. If there are disturbing influences in the system, x and y will only be partially related. The product moment

$$E\{\underline{xy}\} = \int_{-\infty}^{+\infty} \int_{-\infty}^{+\infty} xyf(x,y)dxdy \qquad (20)$$

serves as a measure of correlation between x and y where $E\{\underline{xy}\}$ is called the correlation or expected value of the product of the random variables $\underline{x}$ and $\underline{y}$. If the random variables $\underline{x}$ and $\underline{y}$ are represented by random processes $\underline{x}(t_1)$ and $\underline{x}(t_2)$ respectively, then Eq (20) can be defined as

$$E\{\underline{x}(t_1)\underline{x}(t_2)\} = R(t_1,t_2) \qquad (21)$$

where the function $R(t_1,t_2)$ is called the correlation function or the autocorrelation function of the random process.

If a stationary process is assumed, then instead of the ensemble average in Eq (20), a time average

$$R(x,y) = \lim_{T\to\infty} \frac{1}{T} \int_{0}^{T} x(t)y(t)dt \qquad (22)$$

11

may be written. Eqs (20) and (22) are identical if the process is ergodic, that is, one in which the ensemble statistical properties do not vary with time. All ergodic processes are stationary, but not all stationary processes are ergodic. Under the assumption of ergodicity

$$E\{\underline{xy}\} = R(x,y) \tag{23}$$

If $\underline{x}(t)$ and $\underline{y}(t)$ are represented by $\underline{x}$ and $\underline{y}$ respectively, then $E\{\underline{x}(t)\underline{y}(t)\} = R[x(t)y(t)]$ is called the cross correlation function since it serves as a measure of the correlation of $\underline{x}(t)$ and $\underline{y}(t)$. If $\underline{x}(t)$ and $\underline{y}(t)$ follow each other closely and are of the same sign (i.e., they correlate positively, then $E\{\underline{xy}\}$ (or $R(x,y)$) will accumulate positively. If $\underline{x}(t)$ and $\underline{y}(t)$ follow closely and are of opposite sign (i.e., they correlate negatively), then $E\{\underline{xy}\}$ (or $R(x,y)$) will accumulate negatively. On the other hand, if $\underline{x}(t)$ and $\underline{y}(t)$ vary independently (i.e., uncorrelated) they tend to cancel each other and the $E\{\underline{xy}\}$ (or $R(x,y)$) would approach zero.

If $x(t + \tau)$, which is $x(t)$ delayed by a factor τ, is substituted for $y(t)$, Eq (22) becomes

$$R(x,x) = \lim_{T \to \infty} \frac{1}{T} \int_0^T x(t)x(t + \tau)dt \tag{24}$$

and is called the time autocorrelation function and denoted by $\varphi(\tau)$.

Periodic Functions. If a phenomenon which can be

12

designated by a time history is repetitive with a constant
duration between arbitrarily selected repetitions, then, it
is said to be periodic. The symbolic definition of a peri-
odic function is expressed as $g(t) = g(t + T)$. If T is
the smallest number for which this identity holds, it is
called the period of the function. The relation is also
assumed to hold for all multiples of T. Thus, the law or
description of periodic events is time invariant, and these
events can be classified as noninformative because they are
completely predictable without further observation.

The autocorrelation of a periodic function g(t) is
defined by the expression

$$\varphi(\tau) = \frac{1}{T} \int_{-T/2}^{T/2} g(t)g(t + \tau)dt \tag{25}$$

where

$T = w/2\pi$, period of g(t)

$\tau =$ is the continuous displacement in the interval

$(+\infty, -\infty)$, independent of t

A close examination of the defining equation reveals that
three distinct operations are involved: displacement by an
amount τ, continuous multiplication, and averaging by inte-
gration over a complete period. Essentially, the displace-
ment and averaging provide a means of transforming the func-
tion to a new time domain. This process also eliminates
only phase information, and only the magnitude information
can then be transformed to the frequency domain.

13

The Fourier expansion of $g(t)$ is

$$g(t) = \sum_{n=-\infty}^{+\infty} G(n)e^{-jw_n t} \qquad (26)$$

where

$$G(n) = a_n - jb_n$$

$$= \frac{1}{T} \int_{-T/2}^{T/2} g(t)e^{-jnw_n t} dt \qquad (27)$$

The Fourier expansion of $g(t + \tau)$ is

$$g(t + \tau) = \sum_{n=-\infty}^{+\infty} G(n)e^{-jnw_n(t+\tau)} \qquad (28)$$

Substituting Eq (28) into Eq (25)

$$\varphi(\tau) = \frac{1}{T} \int_{-T/2}^{T/2} g(t) \frac{1}{T} \sum_{n=-\infty}^{+\infty} G(n)e^{jnw_n(t+\tau)} dt \qquad (29)$$

or rearranging Eq (29)

$$\varphi(\tau) = \frac{1}{T} \sum_{n=-\infty}^{+\infty} G(n)e^{jnw_n\tau} \frac{1}{T} \int_{-T/2}^{T/2} g(t)e^{jnw_n t} dt \qquad (30)$$

The integral in Eq (30) is the complex conjugate of Eq (27). Substituting $G^*(n)$ into Eq (3)

$$\varphi(\tau) = \frac{1}{T} \sum_{n=-\infty}^{+\infty} \frac{[G(n)G^*(n)]}{T} e^{jnw_n\tau}$$

$$= \frac{1}{T} \sum_{n=-\infty}^{+\infty} \frac{|G(n)|^2}{T} e^{jnw_n\tau} \qquad (31)$$

14

where $|G(n)|^2 = G(n)G^*(n)$. The autocorrelation function with an argument of zero ($\tau = 0$) is

$$\varphi(0) = \frac{1}{T} \int_{-T/2}^{T/2} g^2(t)\,dt \tag{32}$$

which is the mean square value of $g(t)$. If it is assumed that there is a load resistor of one ohm and that $g(t)$ represents either current or voltage, then the mean square power consumed is the sum of the power contributed by the individual harmonics into which $g(t)$ has been resolved. This is known as Parseval's Theorem for periodic functions.

If $|G(n)|^2 / T$ is defined as the power spectrum $\Phi(n)$, then from Eq (31)

$$\varphi(\tau) = \frac{1}{T} \sum_{n=-\infty}^{+\infty} \Phi(n) e^{jnw_n\tau} \tag{33}$$

and inversely

$$\Phi(n) = \int_{-T/2}^{T/2} \varphi(\tau) e^{-jnw_n\tau}$$

$$= |G(n)|^2 / T \tag{34}$$

Eqs (33) and (34) form the autocorrelation theorem for a periodic function. That is, the autocorrelation function and the power spectrum are Fourier transforms of each other.

In summary, some important properties covered in this section on periodic functions (Ref 6:1166) are:

1. A periodic function can be represented as the

15

summation of discrete, ordered harmonics having
the properties of amplitude and phase relations
in the time domain.

2. These properties can be transformed to the fre-
    quency domain.

3. Autocorrelation transforms only the magnitude
    properties of the unordered harmonics to a new
    time domain.

4. These magnitude properties can be transformed to
    the frequency domain.

Random Functions. If a phenomenon which can be desig-
nated by a time history is repetitive with varying duration
between arbitrarily selected repetitions, then it is said to
be random. Thus, the law or description of random events is
time variant or unordered in time. These events are classi-
fied as informative because they are predictable only in a
statistical sense. Unlike the periodic phenomenon which is
completely predictable from the assumed exact function $g(t)$,
the random phenomenon can only be predicted from an assumed
exact probability density function. The exactness assump-
tion for the periodic function is usually obvious, although
in the end it is dependent on induction. The exactness
assumption for probability densities is not so obvious, and
it is dependent on such concepts as stationarity and ergod-
icity as well as induction. However, these difficulties are
easily removed by defining the autocorrelation function for
the random function as a limiting process for an infinite

16

observation. Thus, the observation must be long enough to establish the exactness of the probability densities involved in correlation, or for lesser lengths it can be assumed that an approximation is made of the exact autocorrelation function.

With the above concepts, the random autocorrelation function can be derived directly from the periodic autocorrelation function by allowing the period to go to infinity. From Eq (25)

$$\varphi(\tau) = \frac{1}{T} \int_{-T/2}^{T/2} g(t)g(t + \tau)dt \qquad (35)$$

As $T \to +\infty$ and $\varphi \to \varphi_1$, the random autocorrelation is given as

$$\varphi_1(\tau) = \lim_{T \to \infty} \frac{1}{2T} \int_{-T}^{T} g_1(t)g_1(t + \tau)dt \qquad (36)$$

where $g_1(t)$ is considered a stationary random function. Since the random function $g_1(t)$ cannot have a periodic component by definition, it can be shown that the random autocorrelation function must decay to zero and is, therefore, aperiodic and finite. Now the $\int_{-\infty}^{+\infty} |\varphi_1(\tau)|d\tau$ is also finite and this satisfies the bounding assumption for a Fourier analysis.

The representation of a random autocorrelation function in the frequency domain can also be derived from the periodic approach. From Eqs (33) and (34)

17

$$\varphi(\tau) = \sum_{n=-\infty}^{+\infty} e^{jnw_n\tau} \frac{1}{T} \int_{-T/2}^{T/2} \varphi(\tau)e^{-jn\tau w_n}dt \qquad (37)$$

As $T \to +\infty$, $1/T \to dw/2\pi$, $nw_n \to w$ and $\varphi(\tau) \to \varphi_1(\tau)$ then

$$\varphi_1(\tau) = \frac{1}{2\pi} \int_{-\infty}^{+\infty} e^{jw\tau}dw \int_{-\infty}^{+\infty} \varphi_1(\tau)e^{-jw\tau}d\tau \qquad (38)$$

As before, the now continuous spectrum of $\varphi_1(\tau)$ is defined by

$$\Phi_1(w) = \int_{-\infty}^{+\infty} \varphi_1(\tau)e^{-jw\tau}d\tau \qquad (39)$$

and it forms a Fourier transform pair, in integral form, with

$$\varphi_1(\tau) = \frac{1}{2\pi} \int_{-\infty}^{+\infty} \Phi_1(w)e^{jw\tau}dw \qquad (40)$$

The physical significance of $\Phi_1(w)$ can be shown by having $\tau = 0$ in Eq (40). Then

$$\varphi_1(0) = \frac{1}{2\pi} \int_{-\infty}^{+\infty} \Phi_1(w)dw \qquad (41)$$

From the defining equation for the autocorrelation function, Eq (36), when $\tau = 0$,

$$\varphi_1(0) = \lim_{T \to \infty} \frac{1}{2T} \int_{-T}^{T} [g_1(t)]^2 dt \qquad (42)$$

18

which is the mean square value of the function $g_1(t)$.
Therefore, from Eqs (41) and (42)

$$\lim_{T\to\infty} \frac{1}{2T} \int_{-T}^{T} [g_1(t)]^2 dt = \frac{1}{2\pi} \int_{-\infty}^{+\infty} \Phi_1(w)\,dw \qquad (43)$$

From Eq (43), $\Phi_1(w)$ is referred to as the power density
spectrum or power spectral density of the random function
$g_1(t)$. If $g_1(t)$ represents a voltage across, or a current
through, a 1 ohm resistor, then the mean value of $g_1(t)$ is
the mean power taken by the load. This mean power consumed
is equal to the integral of $\Phi_1(w)$ with respect to the angu-
lar frequency w over the entire range of frequencies. Con-
sequently, $\Phi_1(w)$ represents the power spectral density of
$g_1(t)$ (Ref 7:58). Since $\Phi_1(w)$ is defined as the Fourier
transform of $\varphi_1(\tau)$, it is a continuous spectrum of the auto-
correlation function.

Some important properties of random functions are:

1. A random function cannot be represented as the
    summation of discrete harmonics, but it can be
    statistically represented as the integrated effect
    of a continuous band of unordered harmonics.

2. Autocorrelation transforms the amplitude proper-
    ties of these harmonic bands to a new finite
    time domain.

3. These amplitude properties can be transformed to
    the frequency domain.

Power Spectral Density

Periodic Functions. The nomenclature, power spectral density, does not actually exist for periodic functions. The correct nomenclature for periodic functions is power spectrum and is represented by Eq (34). In this equation, $|G_1(n)|^2$ is the square of the magnitude spectrum of $g(t)$, the periodic function.

Random Functions. The power spectral density for a random function is given by Eq (39), where $\varphi_1(\tau)$ is the autocorrelation function of a random function. The auto-correlation function is represented by Eq (40) and with Eq (39) forms a Fourier transform pair. However, Eqs (39) and (40) hold only when the random function is stationary in a wide sense (i.e., the random function's statistical properties are invariant to time translation). A more general form for the power spectral density is given as

$$\Phi_1(w) = E\{|G(w)|^2\}$$

$$= E\{|G(w)G^*(w)|\} \tag{44}$$

where

  $G(w)$ = Fourier transform of $g(t)$

  $G^*(w)$ = complex conjugate of $G(w)$

III. Modem Model Description and
Theory of Operation

Introduction

Before an information-bearing signal is transmitted
through a communications channel, some type of modulation
process is typically utilized to produce a signal which can
easily be accommodated by the channel.

The logical choice of modulation techniques is influ-
enced by the characteristics of the message signal, the char-
acteristics of the channel, the performance desired from the
overall communication system, the use to be made of the
transmitted data, and the economic factors which are always
important in practical applications. For this study, the
modulation techniques chosen were influenced by their ease
of modeling and use in present day communications systems.

There are two basic types of modulation: binary and
analog. In the binary case there are three basic ways of
modulating a sinusoidal carrier: variation of its amplitude,
phase, and frequency in accordance with the information
being transmitted. Basically, this corresponds to switch-
ing these three parameters between either of two possible
values. The three basic types of binary modulation are:
amplitude shift keying (ASK), phase shift keying (PSK), and
frequency shift keying (FSK).

In the analog case there are two types of modulation:
continuous-wave and pulse. In continuous-wave modulation,

21

one of the three parameters is again varied proportionally to the message signal such that a one-to-one correspondence exists between the parameter and the message signal. The carrier is usually assumed sinusoidal, though not necessarily so. The three basic types of continuous wave modulation are: amplitude modulation (AM), phase modulation (PM), and frequency modulation (FM).

In analog pulse modulation, some characteristic of a pulse is made to vary in one-to-one correspondence with the message signal. Since the pulse is characterized by three parameters - amplitude, width, and position - there are three types of analog pulse modulation. They are: pulse-amplitude modulation (PAM), pulse-width modulation (PWM), and pulse-position modulation (PPM).

Other modulation techniques exist and are variations and/or combinations of the modulation techniques previously listed. Different modulation techniques can also be realized by changing the carrier signal from sinusoidal to one that is pulsed.

In this study the carrier is assumed sinusoidal and five cases of binary modulation and two cases of analog modulation are considered. The different modulation techniques or modems modeled are:

1. BPSK

2. QPSK

3. BFSK

4. DBFSK

22

5. BASK

6. DSBAM

7. DSBAM-SC

BPSK Modem

In BPSK the phase of the carrier is switched between two values according to the two levels of the digital input signal to the modem. The two values are usually separated by π radians corresponding to the two signal levels. (This is the only choice considered in this report.) This technique is sometimes called phase reversal keying (PRK).

The effect of phase reversal modulation is to produce a double sideband suppressed-carrier amplitude-modulated waveform where the information signal is digital. Thus, the PSK signal can be written as

$$x_i(t) = A_c x_d(t) \cos w_c t \qquad i = 0,1 \qquad (45)$$

where $x_d(t) = (-1)^{b_n}$ and has value +1 or -1 according to the input digital code $(b_n = 0$ or $1)$ during any bit interval having a duration T, A_c is the peak carrier amplitude, and w_c is the carrier frequency. If the carrier frequency, w_c, is an exact multiple of the bit rate, then $w_c = n2\pi/T$, where the bit rate is T^{-1}. The waveforms of the modulated signal, $x_0(t)$ and $x_1(t)$, can be written as

$$x_0(t) = A_c \cos w_c t \qquad (46)$$

$$x_1(t) = -x_0(t) \qquad (47)$$

23

A simple model of a BPSK modem is shown in Figure 4. The switch in Figure 4 operates at a rate determined by the signaling interval, T, of the binary input signal.
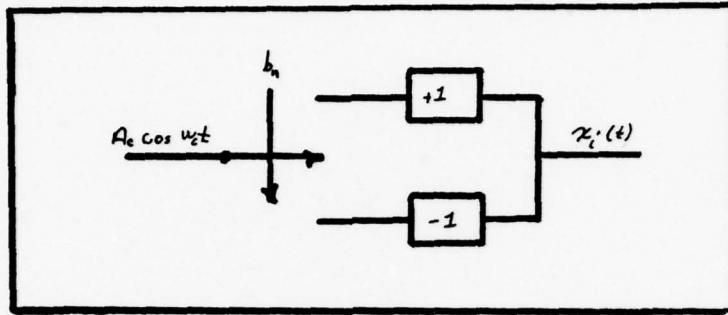
Figure 4. Model for a BPSK Modem

QPSK Modem

With binary digital communications systems, one of only two possible signals can be transmitted during each T-second signaling interval. In an M-ary system, one of M possible signals may be transmitted during each T-second signaling interval, where $M \geq 2$. Thus, binary data transmission is a special case of M-ary data transmission. Each possible transmitted signal of an M-ary message sequence is referred to as a character or symbol. The rate at which M-ary symbols are transmitted through the channel is called baud rate in bauds.

One of the most common M-ary systems is four-phase, or quadriphase shift keying (QPSK).

In general a QPSK modem can be thought of as two BPSK modems in parallel in which the separate carriers are in phase quadrature. Thus, for a given baud rate, T^{-1}, in

24

bauds the rate at which binary digits are sent through the channel for QPSK is double the rate that can be achieved with a binary modem operating at the same signaling rate. Thus, the signal from the QPSK modem has a signaling interval twice that of the binary input signal. The QPSK signal can be written as

$$x_i(t) = x_q(t) + x_p(t) \qquad i = 0,1,2,3 \qquad (48)$$

where

$$x_q(t) = A_c x_{dq}(t) \sin w_c t \qquad (49)$$

and

$$x_p(t) = A_c x_{dp}(t) \cos w_c t \qquad (50)$$

Eq (49) represents the quadrature phase modulated signal and the in-phase modulated signal is represented by Eq (50). The carriers, $\cos w_c t$ and $\sin w_c t$ are modulated by the bit streams $x_{dq}(t)$ and $x_{dp}(t)$ which are obtained by grouping the bits of the binary signal $x_d(t)$ with half the bit period of x_{dq} and x_{dp}, two bits at a time. The values for $x_d(t)$ are -1 or +1 and are determined by the input digital code, b_o. Therefore, from the above discussion, $x_{dq}(t)$ and $x_{dp}(t)$ have values +1 or -1 depending on the digital codes b_n and b_m, respectively. The b_n and b_m digital codes result from the coding of b_o. Thus, $x_{dq}(t) = (-1)^{b_n}$ and $x_{dp}(t) = (-1)^{b_m}$ with b_n and b_m each having value of 0 and 1. Since the phase of the transmitted signal is $\theta_i = \tan^{-1}(x_{dq} / x_{dp})$ it can be seen that θ_i can take on four possible values, $\pm 45^o$ and $\pm 135^o$. Thus, four signals can be obtained as shown

25

by the substitution of Eqs (49) and (50) into Eq (48) when $x_{dq}(t)$ and $x_{dp}(t)$ each have values of +1 or -1.

A simple model of a QPSK modem is shown in Figure 5.
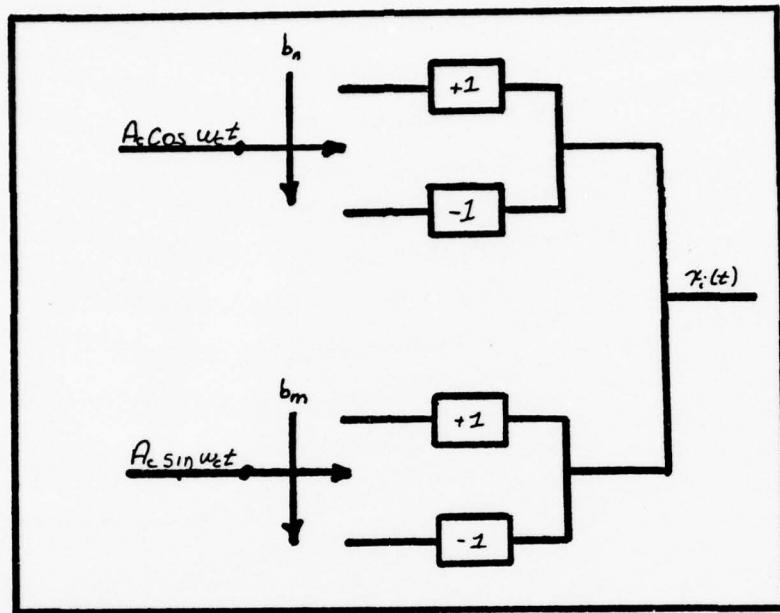
Figure 5. Model for a QPSK Modem

BFSK Modem

Generating a carrier waveform by BFSK consists of switching between two constant frequency sources with the source selected being dependent on the binary input signal which is coded with zeros and ones. Thus, the transmission of a code zero may correspond to a pulse of frequency $w_c + \Delta w$, while a code one selects a frequency $w_c - \Delta w$, where w_c is the carrier frequency and Δw is the peak frequency deviation. Thus, the FSK signal can be written as

$$x_i(t) = A_c \cos (w_c + x_d(t)\Delta w)t \qquad i = 0,1 \qquad (51)$$

26

where $x_d(t) = (-1)^{b_n}$ and has value of +1 or -1 according to the digital code (b_n = 0 or 1) during any bit interval having a duration T, and A_c is the peak carrier amplitude. The waveforms $x_0(t)$ and $x_1(t)$ can be written as

$$x_0(t) = A_c \cos (w_c + \Delta w)t$$

$$= A_c \cos w_1 t \qquad (52)$$

$$x_1(t) = A_c \cos (w_c - \Delta w)t$$

$$= A_c \cos w_2 t \qquad (53)$$

where

$$w_1 = w_c + \Delta w$$

$$w_2 = w_c - \Delta w$$

A simple model of a BFSK modem is shown in Figure 6. The switch operates at a rate determined by the signaling interval, T, of the binary input signal.
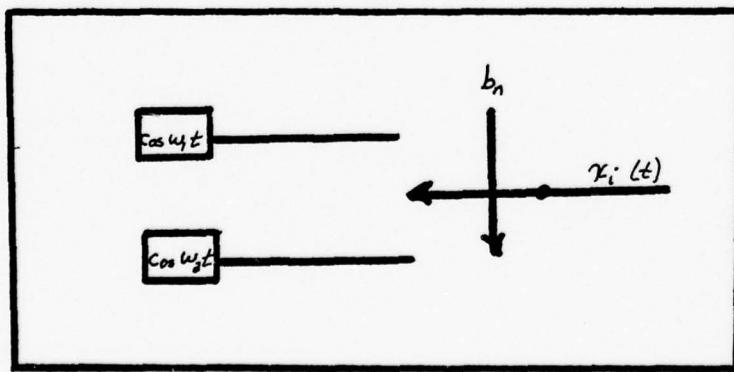
Figure 6. Model for a BFSK Modem

<u>DBFSK</u> <u>Modem</u>

In generating a DBFSK waveform, the binary input data
is encoded (duobinary encoding) before being modulated.
Figure 7 shows one of the ways in which the binary input
signal is encoded.
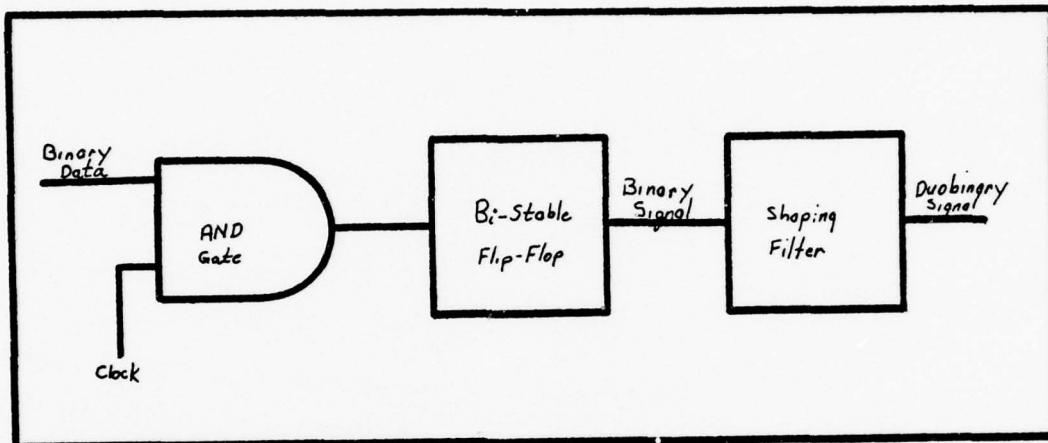
Figure 7. Duobinary Encoder (Ref 5:400)

Binary data pulses are applied to one input of a sim-
ple AND gate, and a stream of binary "clock" pulses of the
same repetition rate as the data pulses is applied to the
other input. Whenever a data space (zero bit) occurs, the
AND gate yields an output pulse which is applied to a "flip-
flop" circuit or bi-stable multivibrator. The multivibrator
has the characteristic of changing its output voltage from
zero to plus or plus to zero, whenever it is triggered by
the AND gate. Thus, for every data space, the output of
the flip-flop changes state. Whenever a data mark is re-
ceived, no change occurs. The binary waveform from the
flip-flop is then passed through a low-pass shaping filter.

Because of the encoding process, the signal now has one very unique property. As it passes through the shaping filter, the waveform is altered so that it tends to occupy three amplitude levels. Superficially, this three-level signal resembles a bipolar signal as shown in Figure 8. This duobinary signal has one unique feature in that the signal cannot transition from one extreme level to the opposite extreme within one bit interval.
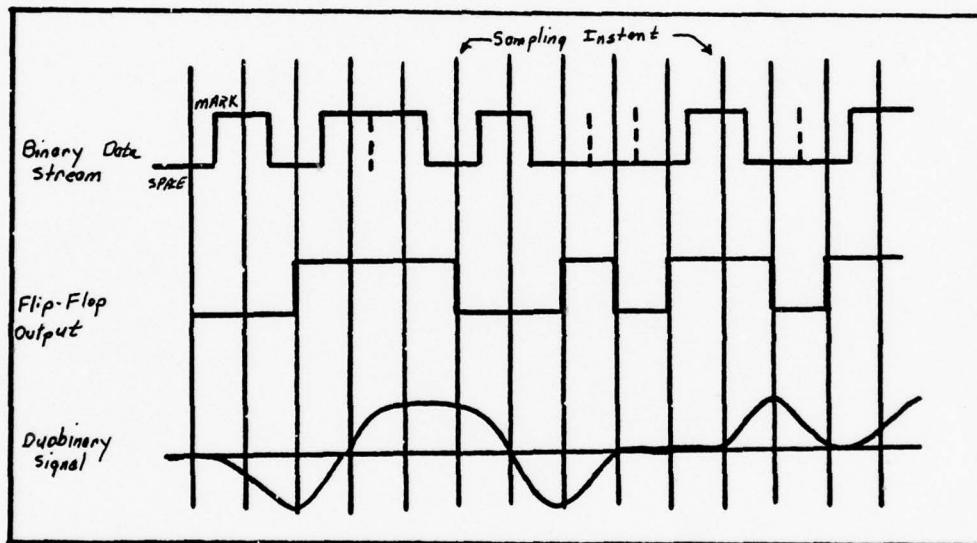
Figure 8. Resulting Waveforms of a Binary Signal Inserted into the Diagram Shown in Figure 7 (Ref 5:400)

A continuous series of input data spaces causes the flip-flop to change state repeatedly, thus creating a series of binary pulses at the data rate. Since this is too fast to pass through the shaping filter, a zero level results. A continuous series of marks results in the flip-flop remaining in whichever state it was in at the beginning of

29

the sequence. The single voltage, tone, or phase by which this marking condition is transmitted will pass through the filter. Since either plus or minus represents a mark, the signal will not change for consecutive marks, but only when a space follows a mark. A second space holds the output in the zero condition, but a mark following the space returns the signal to a mark condition as shown in Figure 8.

The duobinary transformation (Ref 11) used in this study is

$$H(w) = \sqrt{1/2} \cos (wT/2) \tag{54}$$

where T^{-1} is the data rate and $H(w)$ is a transformation in the frequency-domain. Therefore, the duobinary signal of Figure 7 can be represented as

$$z(t) = h(t)x_a(t) \tag{55}$$

where

$z(t)$ = is the duobinary signal

$h(t)$ = is the inverse Fourier transform of $H(w)$

$x_a(t)$ = is the binary input signal

After the input waveform has been encoded, the resulting duobinary signal is modulated using the FSK modulation scheme. However, instead of switching between two constant frequency sources, the switching occurs between three constant frequency sources with the source selected being dependent on the duobinary signal. Since the duobinary signal has three levels (in this case represented by +1, 0,

30

and -1), the transmission of a code +1 corresponds to a pulse of frequency of $w_c + \Delta w$. For a code 0 the frequency is w_c and for a code -1 the frequency is $w_c - \Delta w$. Thus, the DBFSK signal can be written as

$$x_i(t) = A_c \cos (w_c + x_{db}(t)\Delta w)t \qquad i = 0,1,2 \qquad (56)$$

where $x_{db}(t)$ has values +1, 0, and -1, depending on the duo-binary coding of the binary input signal. The waveforms then are

$$x_0(t) = A_c \cos (w_c + \Delta w)t$$

$$= A_c \cos w_1 t \qquad (57)$$

$$x_1(t) = A_c \cos w_c t$$

$$= A_c \cos w_2 t \qquad (58)$$

$$x_2(t) = A_c \cos (w_c - \Delta w)t$$

$$= A_c \cos w_3 t \qquad (59)$$

where

$$w_1 = w_c + \Delta w \text{ when } x_{db}(t) \text{ is } +1$$
$$w_2 = w_c \qquad \text{when } x_{db}(t) \text{ is } 0$$
$$w_3 = w_c + \Delta w \text{ when } x_{db}(t) \text{ is } -1$$

A simple model of a DPFSK modem is shown in Figure 9. The switch operates at a rate determined by the signaling interval, T, of the duobinary input signal.

31
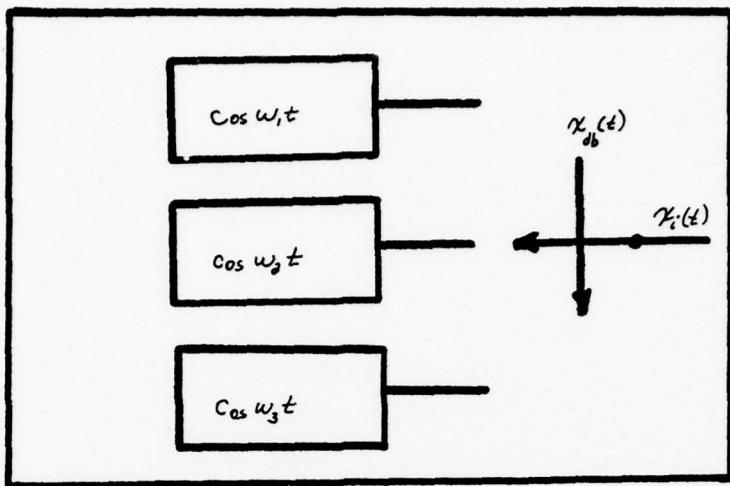
Figure 9.   Model for a DBFSK Modem

BASK Modem

    In BASK the amplitude of a carrier is switched between two levels, usually the extremes of full on and full off. As a result, ASK is sometimes referred to as on-off keying (OOK). The on condition might typically correspond to a code one, while off corresponds to a code zero. Thus, the ASK signal is written as

$$x_i(t) = \frac{A_c}{2}\left[1 + x_d(t)\right]\cos w_c t \quad i = 0,1 \qquad (60)$$

where $x_d(t) = (-1)^{b_n}$ and has value +1 or -1 according to the digital code $(b_n = 0$ or $1)$ during any bit interval having a duration, T, and A_c is the peak carrier amplitude. The "1" in Eq (60) is the dc level added to the digital signal $x_d(t)$. The waveforms $x_0(t)$ and $x_1(t)$ can be written as

$$x_0(t) = A_c \cos w_c t \qquad (61)$$

32

$$x_1(t) = 0 \tag{62}$$

A simple model of a BASK modem is shown in Figure 10. The switch operates at a rate determined by the signaling interval, T, of the binary input signal.
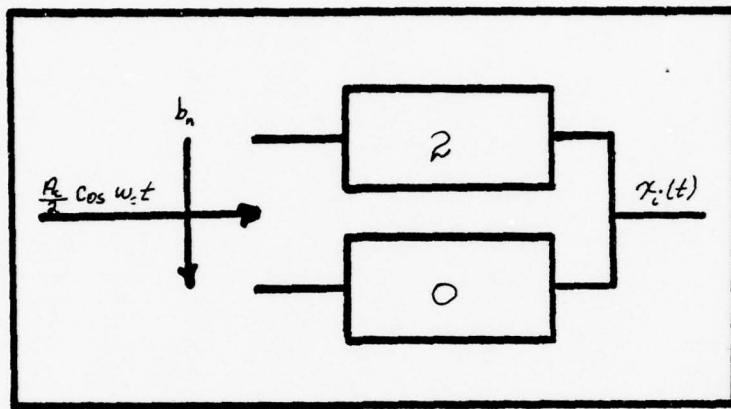
Figure 10.   Model for a BASK Modem

DSBAM Modem

In DSBAM the amplitude of the carrier is varied proportionally to the message signal such that a one-to-one correspondence exists between the carrier amplitude and the message signal. Since DSBAM results when a dc bias is added to the message signal prior to the modulation process, the resulting waveform is

$$x(t) = A_c \left[A + x_m(t) \right] \cos w_c t \tag{63}$$

where

A_c = maximum amplitude of the carrier

w_c = carrier frequency

$x_m(t)$ = analog message signal

33

A   = dc bias added to message signal

A simple model of a DSBAM modem is shown in Figure 11.
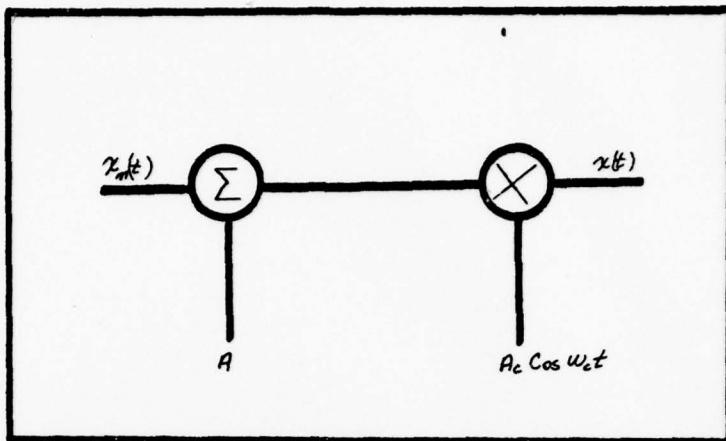
Figure 11.   Model for a DSBAM Modem

DSBAM-SC Modem

The only difference between DSBAM and DSBAM-SC is that in Eq (63), the dc bias, A, is zero. Thus, the resulting DSBAM-SC waveform is represented as

$$x(t) = A_c x_m(t) \cos w_c t \qquad (64)$$

A simple model of a DSBAM-SC modem is shown in Figure 12.
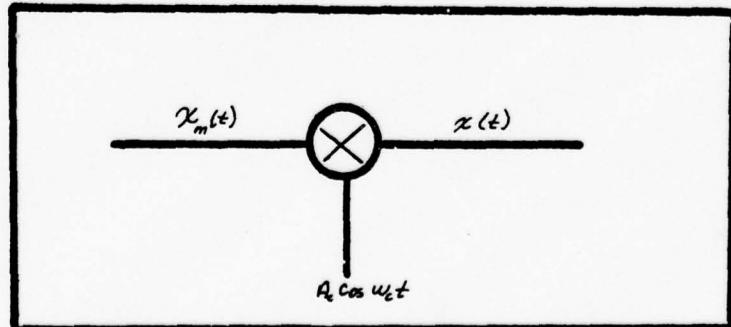
Figure 12.   Model for a DSBAM-SC Modem

IV. Analytical Procedures for
Modem Characterization

Introduction

In this chapter the analytical procedures for characterizing the modems modeled in Chapter III are formulated. Each modem is characterized primarily by determining the power spectral density and secondarily by determining the autocorrelation function (except for the DBFSK, DSBAM, and DSBAM-SC modems) of the output signal, $x_p(t)$, shown in Figure 2.

The input signal to each of the binary modems is a random process and for the binary modems this input has only two possible values, namely, zero and one. The binary signal is a random pulse train with each pulse having period T. A sample pulse is shown in Figure 3. The output signal from each of the binary modems modeled is also a random process.

The input signal to the analog modems is a special periodic function given by (Ref 12:428)

$$a(t) = \gamma \cos w_s t \qquad (65)$$

where

w_s = frequency of the special function and $w_s < w_c$

γ = amplitude factor $0 \leq \gamma \leq 1$

The expected or mean value of the output signal will also be determined (except for DBFSK, DSBAM and DSBAM-SC modems) as it will be needed in determining the autocorrelation function. Once the autocorrelation function is

calculated then it can be determined whether the output signal of the modem being analyzed is a nonstationary or stationary process in the wide sense. A wide sense stationary process is one that has a mean that is constant or zero, and whose second moments are invariant to time translation. This invariance implies that the underlying physical mechanism producing the process in not changing with time. The determination of whether the output signal is a stationary process in the wide sense or a nonstationary process has a bearing on how the autocorrelation is related to the power spectral density. If the process is not stationary then Eq (44) is used instead of Eq (39) to find the power spectral density.

BPSK Modem Characterization

Using the modem model shown in Figure 4 of Chapter III with an input a random pulse train, the output signal of a BPSK modem is represented as

$$\underline{x}_p(t) = \sum_{n=o}^{N} (-1)^{\underline{b}_n} \cos w_c t P(t - nT) \tag{66}$$

where

$$\underline{b}_n \qquad\qquad = \text{random variable equally likely to be one or zero}$$

$$\sum_{n=o}^{N} P(t - nT) = \text{the } n^{th} \text{ signaling interval of the input signal summed over n intervals with each pulse having period T}$$

$$w_c \qquad\qquad = \text{carrier frequency}$$

The mean or expected value of $\underline{x}_p(t)$ is

$$E\{\underline{x}_p(t)\} = E\left\{\sum_{n=o}^{N} (-1)^{\underline{b}_n} \cos w_c tP(t - nT)\right\} \qquad (67)$$

Now using the definition of expectation (Ref 10:138-140), Eq (67) can be expressed as

$$E\{\underline{x}_p(t)\} = \sum_{n=o}^{N} \cos w_c tP(t - nT)E\{(-1)^{\underline{b}_n}\} \qquad (68)$$

since the expectation of a constant times a random variable is the constant times the expectation of the random variable. Therefore, using the given assumption about the input signal having zeros and ones equally likely, the probability P of a one or zero occurring is $P(\underline{b}_n = 1) = P(\underline{b}_n = 0) = 1/2$. Then, substituting in for $\underline{b}_n$, the values zero and one, and using the definition of expectation of a sum of discrete random variables (Ref 10:138)

$$E\{(-1)^{\underline{b}_n}\} = P(\underline{b}_n = 0)(-1)^0 + P(\underline{b}_n = 1)(-1)^1$$

$$= (1/2)(1) + (1/2)(-1)$$

$$= 0 \qquad (69)$$

Therefore, substituting the result of Eq (69) into Eq (68)

$$E\{\underline{x}_p(t)\} = 0 \qquad (70)$$

results in the expected value or mean of the output signal

to be zero

The autocorrelation function of $\underline{x}_p(t)$ using Eq (21) is

$$R(t_1, t_2) = E\{\underline{x}_p(t_1)\underline{x}_p(t_2)\}$$

$$= E\left\{ \sum_{n=o}^{N} \sum_{m=o}^{N} \cos w_c t_1 \cos w_c t_2 P(t_1 - nT) \right.$$

$$\left. P(t_2 - mT)(-1)^{\underline{b}_n}(-1)^{\underline{b}_m} \right\} \qquad (71)$$

and using the definition of expectation, Eq (70) is expressed as

$$R(t_1, t_2) = \sum_{n=o}^{N} \sum_{m=o}^{N} \cos w_c t_1 \cos w_c t_2 P(t_1 - nT)$$

$$P(t_2 - mT)E\{(-1)^{\underline{b}_n}(-1)^{\underline{b}_m}\} \qquad (72)$$

In Eq (72), the output signal, $\underline{x}_p(t)$, is sampled at two different times, t_1 and t_2, which may or may not lie within the same signaling interval, T. The signaling intervals are determined by the values of m and n. Now the $E\{(-1)^{\underline{b}_n}(-1)^{\underline{b}_m}\}$ in Eq (72) is found by referring to Tables I and II.

TABLE I

Comparison of Sample Pulse Values and the
Probability of the Pulses Occurring (n≠m)

Sample Pulse Value		Probability of Occurrence		
$\underline{b}_n$	$\underline{b}_m$	$P(\underline{b}_n)$	$P(\underline{b}_m)$	$P(\underline{b}_n)P(\underline{b}_m)$
0	0	1/2	1/2	1/4
0	1	1/2	1/2	1/4
1	0	1/2	1/2	1/4
1	1	1/2	1/2	1/4

TABLE II

Comparison of Sample Pulse Values and the
Probability of the Pulses Occurring (n=m)

Sample Pulse Value		Probability of Occurrence	
b_n	b_m	$P(b_n)$	$P(b_m)$
0	0	1/2	1/2
1	1	1/2	1/2

These two tables represent the two cases for determining the $E\{(-1)^{b_n}(-1)^{b_m}\}$, namely, when the sample times, t_1 and t_2, occur in different signaling intervals, $n \neq m$, and when the sample times, t_1 and t_2, occur in the same signaling interval, $n = m$. Using the definition for expectation of a sum of discrete random variables and remembering that the pulses are independent, then for the case when $n \neq m$

$$E\{(-1)^{b_n}(-1)^{b_m}\} = E\{(-1)^{b_n}\}E\{(-1)^{b_m}\}$$

$$= P(b_n = 0)P(b_m =))(-1)^0(-1)^0$$

$$+ P(b_n = 0)P(b_m = 1)(-1)^0(-1)^1$$

$$+ P(b_n = 1)P(b_m = 0)(-1)^1(-1)^0$$

$$+ P(b_n = 1)P(b_m = 1)(-1)^1(-1)^1$$

$$= 1/4 - 1/4 - 1/4 + 1/4$$

$$= 0 \tag{73}$$

In the case where n = m, only two conditions occur, namely

when $n = m = 0$ and $n = m = 1$. As a result

$$E\{(-1)^{\underline{b}_n}(-1)^{\underline{b}_m}\} = E\{(-1)^{\underline{b}_n}\}E\{(-1)^{\underline{b}_m}\}$$

$$= P(\underline{b}_n = 0)(-1)^0(-1)^0$$

$$+ P(\underline{b}_n = 1)(-1)^1(-1)^1$$

$$= 1/2 + 1/2$$

$$= 1 \qquad (74)$$

Therefore, substituting the result of Eq (73) into Eq (72), the autocorrelation function

$$R(t_1, t_2) = 0 \qquad (75)$$

when $n \neq m$ or when t_1 and t_2 are not in the same signaling interval. Substituting the result of Eq (74) into Eq (72)

$$R(t_1, t_2) = \sum_{n=o}^{N} \sum_{m=o}^{N} \cos w_c t_1 \cos w_c t_2 P(t_1 - nT) P(t_2 - mT) \qquad (76)$$

when $n = m$ or when t_1 and t_2 are in the same signaling interval. Since $n = m$ in Eq (76), it can be reduced to

$$R(t_1, t_2) = \cos w_c t_1 \cos w_c t_2 \qquad (77)$$

as the term, $\sum_{n=o}^{N} \sum_{m=o}^{N} P(t_1 - nT) P(t_2 - nT) = 1$.

Combining Eqs (75) and (77)

40

$$R(t_1, t_2) = \begin{cases} 0 & \text{when } t_1 \text{ and } t_2 \text{ are not in} \\ & \text{the same signaling interval} \\ \cos w_c t_1 \cos w_c t_2 & \text{when } t_1 \text{ and } t_2 \text{ are in the} \\ & \text{same signaling interval} \end{cases} \tag{78}$$

From the definition of a wide-sense stationary process, it can be seen that $\underline{x}_p(t)$ is nonstationary as it is time dependent. Therefore, Eq (44) is used to find the power spectral density of the output signal from the modem.

In order to find the power spectral density, the output signal $\underline{x}_p(t)$ must be transformed to the frequency-domain. Using the properties of the Fourier transform outlined in Chapter II, the frequency-domain transform of $\underline{x}_p(t)$ is represented as

$$\underline{X}_p(w) = F\left[\underline{x}_p(t)\right]$$

$$= F\left[\sum_{n=o}^{N} (-1)^{b_n} \cos w_c t P(t - nT)\right] \tag{79}$$

where

$$F\left[\cos w_c t\right] = 1/2\delta(w + w_c) + 1/2\delta(w - w_c) \tag{80}$$

and

$$F\left[P(t - nT)\right] = \frac{T \sin (wT/2)}{(wT/2)} e^{-jwT(n+1/2)} \tag{81}$$

Therefore,

41

$$\underline{X}_p(w) = \sum_{n=o}^{N} (-1)^{\underline{b}_n} (T/2) \left[\frac{\sin \left[(w + w_c)T/2\right]}{(w + w_c)T/2} e^{-jT(w+w_c)(n+1/2)} \right.$$

$$\left. + \frac{\sin \left[(w - w_c)T/2\right]}{(w - w_c)T/2} e^{-jT(w-w_c)(n+1/2)} \right] \qquad (82)$$

Now from Eq (44)

$$|\underline{X}_p(w)|^2 = \underline{X}_p(w)\underline{X}_p^*(w) \qquad (83)$$

and

$$E\{|\underline{X}_p(w)|^2\} = E\{\underline{X}_p(w)\underline{X}_p^*(w)\} \qquad (84)$$

where $\underline{X}_p^*(w)$ is the complex conjugate of $\underline{X}_p(w)$. Since $\underline{x}_p(t)$ was assumed real, then $\underline{X}_p^*(w)$ is just the conjugate of the real process $\underline{X}_p(w)$. The power spectral density is then

$$E\{|\underline{X}_p(w)|^2\} = E \left\{ \sum_{n=o}^{N} \sum_{m=o}^{N} (-1)^{\underline{b}_n}(-1)^{\underline{b}_m} (T^2/4) \left[\rule{0pt}{20pt} \right. \right.$$

$$\frac{\sin \left[(w + w_c)T/2\right]}{(w + w_c)T/2} e^{-jT(w+w_c)(n+1/2)}$$

$$\frac{\sin \left[(w + w_c)T/2\right]}{(w + w_c)T/2} e^{-jT(w+w_c)(m+1/2)} + \frac{\sin \left[(w - w_c)T/2\right]}{(w - w_c)T/2}$$

$$\frac{\sin \left[(w - w_c)T/2\right]}{(w - w_c)T/2} e^{-jT(w-w_c)(n+1/2)} e^{-jT(w-w_c)(m+1/2)} \left. \left. \rule{0pt}{20pt} \right] \right\} \qquad (85)$$

or combining terms

$$E\{|\underline{X}_p(w)|^2\} = \sum_{n=o}^{N} \sum_{m=o}^{N} T^2/4 \Bigg[$$

$$\frac{\sin^2[(w+w_c)T/2]}{[(w+w_c)T/2]^2} e^{-jT(w+w_c)(n+1/2)} e^{-jT(w+w_c)(m+1/2)}$$

$$+ \frac{\sin^2[(w-w_c)T/2]}{[(w-w_c)T/2]^2} e^{-jT(w-w_c)(n+1/2)} e^{-jT(w-w_c)(m+1/2)} \Bigg]$$

$$E\{(-1)^{\underline{b}_n}(-1)^{\underline{b}_m}\} \qquad (86)$$

The cross-terms resulting from the product of $\underline{X}_p(w)$ and $\underline{X}_p^*(w)$ are considered to be zero since it was initially assumed that $X(w + w_c)$ and $X(w - w_c)$ do not overlap. From Eq (86) it can be seen that two cases must be considered in determining the power spectral density, namely, when $n \neq m$ and when $n = m$. From Eq (73) it was shown that $E\{(-1)^{\underline{b}_n}(-1)^{\underline{b}_m}\} = 0$ when $n \neq m$. Therefore, substituting this result in Eq (86)

$$E\{|\underline{X}_p(w)|^2\} = 0 \qquad (87)$$

when $n \neq m$. Similarily, substituting the result of Eq (74) into Eq (86) results in

$$E\{|\underline{X}_p(w)|^2\} = \sum_{n=o}^{N} \sum_{m=o}^{N} T^2/4 \left[\frac{\sin^2[(w+w_c)T/2]}{[(w+w_c)T/2]^2} \right.$$

$$+ \frac{\sin^2 \left[(w - w_c)T/2 \right]}{\left[(w - w_c)T/2 \right]^2} \Bigg] \qquad (88)$$

when n = m. However, since m = n, Eq (88) can be reduced to

$$E\{ | \underline{X}_p(w) |^2 \} = \frac{NT^2}{4} \Bigg[\frac{\sin^2 \left[(w + w_c)T/2 \right]}{\left[(w - w_c)T/2 \right]^2}$$

$$+ \frac{\sin^2 \left[(w - w_c)T/2 \right]}{\left[(w - w_c)T/2 \right]^2} \Bigg] \qquad (89)$$

Thus, the power spectral density of the output signal of a BPSK modem is given by Eq (89).

QPSK Modem Characterization

Using the modem model shown in Figure 4 of Chapter III and recalling that a QPSK modem can be thought of as two BPSK modems in parallel, then the output of a QPSK modem is represented as

$$\underline{x}_p(t) = \underline{x}_{p1}(t) + \underline{x}_{p2}(t) \qquad (90)$$

where

$$\underline{x}_{p1}(t) = \sum_{n=o}^{N} (-1)^{b_n} \cos w_c t P(t - 2nT) \qquad (91)$$

and is the in-phase component of $\underline{x}_p(t)$, and

$$\underline{x}_{p2}(t) = \sum_{m=o}^{N} (-1)^{b_m} \sin w_c t P(t - 2mT) \qquad (92)$$

44

is the quadrature component of $\underline{x}_p(t)$. The factor of 2 in the terms $P(t - 2nT)$ and $P(t - 2mT)$ of Eqs (83) and (84), respectively, results from the forming of the two bit streams, $x_{p1}(t)$ and $x_{p2}(t)$, from the binary input signal. The signaling interval for the bit streams, $x_{p1}(t)$ and $x_{p2}(t)$ is double that of the input signaling interval (Ref 13:336). Since $\underline{x}_{p1}(t)$ is independent of $\underline{x}_{p2}(t)$, the mean value, auto-correlation, and power spectral density of each of these processes can be calculated independently. Since Eq (91) is similar to Eq (64), with the only difference being the factor of 2 in the term $P(t - 2nT)$ in Eq (58), then the mean value and autocorrelation calculated for $\underline{x}_p(t)$ in the section on BPSK Modem Characterization is the same for $\underline{x}_{p1}(t)$ since the term $P(t - 2nT)$ is a constant for these calculations. Additionally, Eq (92) differs from Eq (66) only in the factor of 2 in the term $P(t - 2mT)$ and in the carrier term of $\sin w_c t$. However, in the calculation of the mean value, the carrier term is constant, therefore, the mean value for $\underline{x}_{p2}(t)$ is that of Eq (70). Therefore, the mean of $\underline{x}_p(t)$ in Eq (90) is zero since the mean of $\underline{x}_{p1}(t)$ and $\underline{x}_{p2}(t)$ are both zero.

The autocorrelation function of Eq (92) is the same as that of Eq (72) with the term $\sin w_c t_1 \sin w_c t_2$ substituted in for $\cos w_c t_1 \cos w_c t_2$. Therefore, the autocorrelation function of Eq (92) is

$$R(t_1, t_2) = \begin{cases} 0 & \text{when } t_1 \text{ and } t_2 \text{ are not in} \\ & \text{the same signaling interval} \\ \sin w_c t_1 \sin w_c t_2 & \text{when } t_1 \text{ and } t_2 \text{ are in the} \\ & \text{same signaling interval} \end{cases}$$

$$(93)$$

Therefore, the autocorrelation function of $\underline{x}_p(t)$ in Eq (90) is

$$R(t_1, t_2) = \begin{cases} 0 & \text{when } t_1 \text{ and } t_2 \text{ are not in} \\ & \text{the same signaling interval} \\ \cos w_c t_1 \cos w_c t_2 & \text{when } t_1 \text{ and } t_2 \text{ are in the} \\ + \sin w_c t_1 \sin w_c t_2 & \text{same signaling interval} \end{cases}$$

$$(94)$$

which indicates that $\underline{x}_p(t)$ is a nonstationary process in a wide-sense. As a result, Eq (44) is used to find the power spectral density which is represented as

$$E\{|\underline{X}_p(w)|^2\} = E\{\underline{X}_p(w)\underline{X}_p^*(w)\}$$

$$= E\{[\underline{X}_{p1}(w) + \underline{X}_{p2}(w)][\underline{X}_{p1}^*(w) + \underline{X}_{p2}^*(w)]\} \quad (95)$$

Eq (95) is found by transforming Eq (90) from the time-domain to the frequency-domain and multiplying this result by its complex conjugate. Eq (95) is reduced to

$$E\{|\underline{X}_p(w)|^2\} = E\{\underline{X}_{p1}(w)\underline{X}_{p1}^*(w) + \underline{X}_{p2}(w)\underline{X}_{p2}^*(w)\} \quad (96)$$

and the product of cross terms, $\underline{X}_{p2}(w)X_{p1}^*(w)$ and $\underline{X}_{p2}^*(w)\underline{X}_{p1}(w)$ are considered zero as a result of assuming that the negative

46

frequency terms and positive frequency terms do not overlap. Using the definition of expectation of a sum of two independent processes, Eq (93) is represented as

$$E\{|\underline{X}_p(w)|^2\} = E\{\underline{X}_{p1}(w)\underline{X}_{p1}^*(w)\} + E\{\underline{X}_{p2}(w)\underline{X}_{p2}^*(w)\} \quad (97)$$

The power spectral density of the first term in Eq (97) is similar to that calculated in the section on BPSK Modem Characterization. This can be seen, since the transformation of Eq (91) is that of Eq (82) with T = 2T. Making the necessary substitutions and using Eqs (84), (85), and (86), the power spectral density of the first term in Eq (97) is equal to that of Eq (89) with T = 2T.

The frequency-domain transformation of Eq (92) is found by using

$$F\left[\sin w_c t\right] = \frac{j}{2}\,\delta\,(w + w_c) - \frac{j}{2}\,\delta\,(w - w_c) \quad (98)$$

and multiplying this result with that of Eq (81) with T = 2T and the term $\sum\limits_{n=o}^{N} (-1)^{\underline{b}_m}$. The transformation of Eq (92) is then

$$\underline{X}_{p2}(w) = \sum_{n=o}^{N} (-1)^{\underline{b}_m}(T)j\left[\frac{\sin\left[(w + w_c)T\right]}{(w + w_c)T}\,e^{-jT(w+w_c)(2n+1)}\right.$$

$$\left. - \frac{\sin\left[(w - w_c)T\right]}{(w - w_c)T}\,e^{-jT(w-w_c)(2m+1)}\right] \quad (99)$$

Using the procedure outlined in the section on BPSK Modem

Characterization on finding the power spectral density, the second term in Eq (97) has power spectral density equal to that of the first term. Therefore, the power spectral density of $\underline{x}_p(t)$ in Eq (90) is

$$
= NT^2 \left[\frac{\sin^2\left[(w + w_c)T\right]}{\left[(w + w_c)T\right]^2} + \frac{\sin^2\left[(w - w_c)T\right]}{\left[(w - w_c)T\right]^2} \right]
$$

$$
+ NT^2 \left[\frac{\sin^2\left[(w + w_c)T\right]}{\left[(w + w_c)T\right]^2} + \frac{\sin^2\left[(w - w_c)T\right]}{\left[(w - w_c)T\right]^2} \right]
$$

$$
= 2NT^2 \left[\frac{\sin^2\left[(w + w_c)T\right]}{\left[(w + w_c)T\right]^2} + \frac{\sin^2\left[(w - w_c)T\right]}{\left[(w - w_c)T\right]^2} \right] \quad (100)
$$

BFSK Modem Characterization

Using the modem model shown in Figure 6 of Chapter III with an input a random pulse train, the output signal of a BFSK modem is represented as

$$
\underline{x}_p(t) = \sum_{n=o}^{N} \cos\left(w_c + (-1)^{b_n}\Delta w\right)tP(t - nT) \quad (101)
$$

where

$\underline{b}_n$ = random variable equally likely to be one or zero

Δw = frequency deviation from w_c

$\sum_{n=o}^{N} P(t - nT)$ = the nth signaling interval of the input signal summed over n intervals with each pulse having period T

w_c = carrier frequency

The mean or expected value of $\underline{x}_p(t)$ is

$$E\{\underline{x}_p(t)\} = E\left\{\sum_{n=o}^{N} P(t - nT) \cos(w_c + (-1)^{b_n}\Delta w)t\right\}$$

$$= \sum_{n=o}^{N} P(t - nT)E\left\{\cos(w_c + (-1)^{b_n}\Delta w)t\right\} \quad (102)$$

Using a trigonometric identity to expand the cosine argument, (i.e., $\cos(u + v) = \cos u \cos v - \sin u \sin v$) Eq (102) reduces to

$$E\{\underline{x}_p(t)\} = \sum_{n=c}^{N} P(t - nT)E\{\cos w_c t \cos(-1)^{b_n}\Delta wt$$

$$- \sin w_c t \sin(-1)^{b_n}\Delta wt\}$$

$$= \sum_{n=o}^{N} P(t - nT)\left[(\cos w_c t)E\{\cos(-1)^{b_n}t\Delta w\}\right.$$

$$\left. - (\sin w_c t)E\{\sin(-1)^{b_n}\Delta wt\}\right] \quad (103)$$

Now substituting in the values of zero and one for $\underline{b}_n$ and evaluating, Eq (103) reduces to

$$E\{\underline{x}_p(t)\} = \sum_{n=o}^{N} P(t - nT) \cos w_c t \cos \Delta wt \quad (104)$$

which is the mean value of $\underline{x}_p(t)$.

Now the autocorrelation function of $\underline{x}_p(t)$ using Eq

49

(21) is

$$R(t_1, t_2) = E\{\underline{x}_p(t_1)\underline{x}_p(t_2)\}$$

$$= E\{\Sigma \; \Sigma \; P(t_1 - nT)P(t_2 - mT) \cos (w_c$$

$$+ (-1)^{b_n}\Delta w)t_1 \cos (w_c + (-1)^{b_m}\Delta w)t_2\}$$

$$= \sum_{n=o}^{N} \sum_{m=o}^{N} P(t_1 - nT)P(t_2 - mT)E\{\cos (w_c$$

$$+ (-1)^{b_n}\Delta w)t_1 \cos (w_c + (-1)^{b_m}\Delta w)t_2\} \quad (105)$$

In Eq (105), $\underline{x}_p(t)$ is sampled in the same manner as is $\underline{x}_p(t)$ in Eq (72).

The BFSK autocorrelation function, Eq (105), is determined using a procedure similar to that used in determining the BPSK autocorrelation function, Eq (72). In determining the autocorrelation function of Eq (105), two cases are considered. The first case is when the sample times, t_1 and t_2, are not in the same signaling interval, $n \neq m$. The second case is when the sample times, t_1 and t_2, are in the same signaling interval, $n = m$. With the use of Tables I and II, the definition and properties of expectation and the procedures for evaluating Eq (73), the autocorrelation function of Eq (105) is given as

$$R(t_1, t_2) = 0 \qquad (106)$$

when $n \neq m$ and

50

$$R(t_1, t_2) = \sin w_c t_1 \sin w_c t_2 \sin \Delta w t_1 \sin \Delta w t_2$$

$$+ \cos w_c t_1 \cos w_c t_2 \cos \Delta w t_1 \cos \Delta w t_2 \qquad (107)$$

when $n = m$. Combining Eqs (106) and (107)

$$R(t_1, t_2) = \begin{cases} \cos w_c t_1 \cos w_c t_2 \cos \Delta w t_1 \text{ when } t_1 \text{ and } t_2 \text{ are} \\ \qquad\qquad\qquad\qquad \cos \Delta w t_2 \text{ in the same sig-} \\ + \sin w_c t_1 \sin w_c t_2 \sin \Delta w t_1 \text{ naling interval} \\ \qquad\qquad\qquad\qquad \sin \Delta w t_2 \\ 0 \qquad\qquad\qquad\qquad\qquad \text{when } t_1 \text{ and } t_2 \text{ are} \\ \qquad\qquad\qquad\qquad\qquad\quad \text{not in the same} \\ \qquad\qquad\qquad\qquad\qquad\quad \text{signaling interval} \end{cases}$$
$$(108)$$

Since Eq (108) indicates that $\underline{x}_p(t)$ is not a wide sense stationary process, Eq (44) is used to determine the power spectral density. The power spectral density of $\underline{x}_p(t)$ is represented as

$$E\{|\underline{X}_p(w)|^2\} = E\{\underline{X}_p(w)\underline{X}_p^*(w)\} \qquad (109)$$

where $\underline{X}_p(w)$ is the Fourier transform of Eq (101) in the frequency-domain. $\underline{X}_p^*(w)$ is the complex conjugate of $\underline{X}_p(w)$. With $\underline{w}_n = (w_c + (-1)^{b_n} \Delta w)$ in Eq (101), the Fourier transform of $\underline{x}_p(t)$ is represented as

$$\underline{X}_p(w) = \sum_{n=0}^{N} T/2 \left[\frac{\sin[(w + \underline{w}_n)T/2]}{(w + \underline{w}_n)T/2} e^{-jT(w+\underline{w}_n)(n+1/2)} \right.$$

$$+ \frac{\sin\left[(w - \underline{w}_n)T/2\right]}{(w - \underline{w}_n)T/2} e^{-jT(w-\underline{w}_n)(n+1/2)} \Bigg] \qquad (110)$$

Substituting Eq (110) and its complex conjugate into Eq (109), the power spectral density of $\underline{x}_p(t)$ is

$$E\{|\underline{X}_p(w)|^2\} = \sum_{n=o}^{N} \sum_{m=o}^{N} T^2/4 \Bigg[E \Bigg\{ \frac{\sin\left[(w + \underline{w}_n)T/2\right]}{(w + \underline{w}_n)T/2}$$

$$\frac{\sin\left[(w + \underline{w}_m)T/2\right]}{(w + \underline{w}_m)T/2} e^{-jT(w+\underline{w}_n)(n+1/2)} e^{-jT(w+\underline{w}_m)(m+1/2)}$$

$$+ \frac{\sin\left[(w - \underline{w}_n)T/2\right]}{(w - \underline{w}_n)T/2}$$

$$\frac{\sin\left[(w - \underline{w}_n)T/2\right]}{(w - \underline{w}_m)T/2} e^{-jT(w-\underline{w}_n)(n+1/2)} e^{-jT(w-\underline{w}_m)(m+1/2)} \Bigg\} \Bigg]$$

$$(111)$$

The cross-terms resulting from Eq (109) are assumed zero and are based on a similar assumption made in deriving Eq (86). Again, two cases must be considered in determining the power spectral density, namely, when $n \neq m$ and $n = m$. After performing the necessary mathematical manipulations, the power spectral density of $\underline{x}_p(t)$ is

$$E\{|\underline{X}(w)|^2\} = \frac{T^2 N}{8} \Bigg[\frac{\sin^2\left[(w \pm w_1)T/2\right]}{\left[(w \pm w_1)T/2\right]^2}$$

52

$$+ \frac{\sin^2 \left[(w \pm w_2)T/2 \right]}{\left[(w \pm w_2)T/2 \right]^2} \Bigg] \tag{112}$$

where

$$w_1 = w_c + \Delta w$$

$$w_2 = w_c - \Delta w$$

The carrier frequencies, w_1 and w_2, are those indicated in Eqs (52) and (53), respectively.

DBFSK Modem Characterization

Using the modem model shown in Figure 9 of Chapter III with the input a random pulse train encoded as a duobinary signal, the output of a DBFSK modem is represented as

$$\underline{x}_p(t) = \sum_{n=o}^{N} h(t)P(t - nT) \cos (w_c + \underline{x}_{db}(t)\Delta w)t \tag{113}$$

where

$$h(t) = \text{the duobinary transformation}$$

$$\underline{x}_{db}(t) = \text{random process having value of 1, 0, and -1, but not equally likely}$$

$$\sum_{n=o}^{N} P(t - nT) = \text{the } n^{th} \text{ signaling interval}$$

$$w_c = \text{carrier frequency}$$

From information published on duobinary encoding (Refs 8:214-218, 11:126-130) and digital transmission (Ref 2:1501-1511), the process $\underline{x}_p(t)$ is nonstationary. Therefore, the power spectral density is found using Eq (44). Using Eq (81), the Fourier transform of $P(t - nT)$; Eq (54), the

53

Fourier transform of h(t); and the Fourier Transform of
cos $[w_c + \underline{x}_{db}(t)\Delta w]t$; the Fourier transform of Eq (113)
is

$$
\underline{X}_p(w) = \sum_{n=o}^{N} \sqrt{1/2}\ (T/2) \left[\cos\left[(w + \underline{w}_n)T/2\right] \right.
$$

$$
\frac{\sin\left[(w + \underline{w}_n)T/2\right]}{(w + \underline{w}_n)T/2}\ e^{-jT(w+\underline{w}_n)(n+1/2)}
$$

$$
+\ \frac{\cos\left[(w - \underline{w}_n)T/2\right]}{(w - \underline{w}_n)T/2}\ \sin\left[(w - \underline{w}_n)T/2\right]\ e^{-jT(w-\underline{w}_n)(n+1/2)} \left. \right]
$$

$$(114)$$

where the substitution, $\underline{w}_n = w_c + \underline{x}_{db}(t)\Delta w$, in Eq (113)
was made prior to taking the Fourier transform of cos
$[w + \underline{x}_{db}(t)\Delta w]t$. Substituting into Eqs (83) and (84),
the power spectral density is

$$
E\{|\underline{X}_p(w)|^2\} = E \left\{ \sum_{n=o}^{N} \sum_{m\neq o}^{N} T^2/8 \left[\cos\left[(w + \underline{w}_n)T/2\right] \right. \right.
$$

$$
\cos\left[(w + \underline{w}_m)T/2\right]\ \frac{\sin\left[(w + \underline{w}_n)T/2\right]}{(w + \underline{w}_n)T/2}
$$

$$
\frac{\sin\left[(w + \underline{w}_m)T/2\right]}{(w + \underline{w}_m)T/2}\ e^{-jT(w+\underline{w}_n)(n+1/2)}\ e^{-jT(w+\underline{w}_m)(m+1/2)}
$$

$$+ \quad \cos\left[(w - \underline{w}_n)T/2\right] \cos\left[(w - \underline{w}_m)T/2\right] \frac{\sin\left[(w - \underline{w}_n)T/2\right]}{(w - \underline{w}_n)T/2}$$

$$\frac{\sin\left[(w - \underline{w}_m)T/2\right]}{(w - \underline{w}_m)T/2} \, e^{-jT(w-\underline{w}_n)(n+1/2)} \, e^{-jT(w-\underline{w}_m)(m+1/2)} \Bigg] \Bigg\}$$

$$(115)$$

Again, the cross-terms are assumed zero. With $\underline{w}_n = w_c$ + $\underline{x}_{db}(t)\Delta w$ and with $\underline{x}_{db}(t)$ having values of +1, 0, and -1, then $w_n = w_c + \Delta w$ when $x_{db}(t) = +1$; $w_n = w_c$ when $x_{db}(t) = 0$; and $w_n = w_c - \Delta w$ when $x_{db}(t) = -1$. Therefore, the three values of $\underline{x}_{db}(t)$ will result in $\underline{w}_n$ having three values. The probability, P, of the occurrence of the levels of the duobinary signal are given as $P(+1) = P(-1) = 1/4$ and the $P(0) = 1/2$ (Ref 8:218).

From Eq (115) it can be seen that two cases must be considered in determining the power spectral density, namely, when $n \neq m$ and when $n = m$. After performing the necessary mathematical manipulations, the power spectral density of $\underline{x}_p(t)$ is

$$E\{|\underline{X}_p(w)|^2\} = \frac{NT^2}{16} \left[\frac{\sin^2\left[(w \pm w_1)T/2\right]}{\left[(w \pm w_1)T/2\right]^2} \right.$$

$$\left. + \frac{2 \sin^2\left[(w \pm w_2)T/2\right]}{\left[(w \pm w_2)T/2\right]^2} \right.$$

$$+ \frac{\sin^2\left[(w \pm w_2)T/2\right]}{\left[(w \pm w_2)T/2\right]^2}\Bigg] \tag{116}$$

where

$$w_1 = w_c + \Delta w$$
$$w_2 = w_c$$
$$w_3 = w_c - \Delta w$$

The carrier frequencies, w_1, w_2, and w_3, are those indicated in Eqs (57), (58), and (59).

BASK Modem Characterization

Using the modem model shown in Figure 10 in Chapter III with an input a random pulse train, the output signal of a BASK modem is represented as

$$\underline{x}_p(t) = \left[1 + \sum_{n=0}^{N} (-1)^{\underline{b}_n} P(t - nT)\right] \cos w_c t \tag{117}$$

The mean or expected value of $\underline{x}(t)$ is

$$E\{\underline{x}_p(t)\} = E\left\{\left[1 + \sum_{n=0}^{N} (-1)^{\underline{b}_n} P(t - nT)\right] \cos w_c t\right\}$$

$$= \cos w_c t + \sum_{n=0}^{N} P(t - nT) \cos w_c t \, E\{(-1)^{\underline{b}_n}\} \tag{118}$$

From Eq (69), $E\{(-1)^{\underline{b}_n}\} = 0$, therefore, the expected or mean value of $\underline{x}_p(t)$ is

$$E\{\underline{x}_p(t)\} = \cos w_c t \tag{119}$$

The autocorrelation function of $\underline{x}_p(t)$ using Eq (21) is

$$R(t_1, t_2) = E\{\underline{x}_p(t_1)\underline{x}_p(t_2)\}$$

$$= E\left\{ [1 + \sum_{n=o}^{N} (-1)^{\underline{b}_n} P(t_1 - nT)] \cos w_c t_1 \right.$$

$$\left. [1 + \sum_{m=o}^{N} (-1)^{\underline{b}_m} P(t_2 - mT)] \cos w_c t_2 \right\}$$

$$= \cos w_c t_1 \cos w_c t_2 + \sum_{n=o}^{N} \sum_{m=o}^{N} P(t_1 - nT) P(t_2 - mT)$$

$$\cos w_c t_1 \cos w_c t_2 \, E\{(-1)^{\underline{b}_n}(-1)^{\underline{b}_m}\} \qquad (120)$$

Using the results of Eqs (73) and (74), the autocorrelation function, Eq (120), is

$$R(t_1, t_2) = \begin{cases} \cos w_c t_1 \cos w_c t_2 \text{ when } t_1 \text{ and } t_2 \text{ are not in} \\ \qquad\qquad\qquad\qquad \text{ the same signaling interval} \\ 2 \cos w_c t_1 \cos w_c t_2 \text{ when } t_1 \text{ and } t_2 \text{ are in the} \\ \qquad\qquad\qquad\qquad \text{ same signaling interval} \end{cases}$$
$$(121)$$

Since $\underline{x}_p(t)$ is a nonstationary process, Eq (44) is used to find the power spectral density. The Fourier transform of Eq (117) is

$$\underline{X}_p(w) = 1/2 \, \delta \, (w + w_c) + 1/2 \, \delta \, (w - w_c)$$

$$+ \sum_{n=o}^{N} (-1)^{b_m}(T/2) \; \frac{\sin\left[(w + w_c)T/2\right]}{(w + w_c)T/2} \; e^{-jT(w+w_c)(n+1/2)}$$

$$+ \sum_{n=o}^{N} (-1)^{b_n}(T/2) \; \frac{\sin\left[(w - w_c)T/2\right]}{(w - w_c)T/2} \; e^{-jT(w-w_c)(n+1/2)} \qquad (122)$$

where the term $\; 1/2 \left[\delta(w + w_c) + \delta(w - w_c)\right] \;$ is the Fourier transform of product of the carrier signal, $\cos w_c t$, and the dc bias, 1.

Substituting Eq (122) and its complex conjugate into Eq (44) and using the results from Eqs (86), (87), and (88), the power spectral density is given as

$$E\{|\underline{X}_p(w)|^2\} = 1/4 \; \delta \; (w + w_c) + 1/4 \; \delta \; (w - w_c)$$

$$+ \frac{NT^2}{4} \left[\frac{\sin^2\left[(w + w_c)T/2\right]}{\left[(w + w_c)T/2\right]^2} + \frac{\sin^2\left[(w - w_c)T/2\right]}{\left[(w - w_c)T/2\right]^2} \right] \qquad (123)$$

The first two terms in Eq (123) are delta functions located at the carrier frequencies, w_c and $-w_c$, and have weight 1/2.

DSBAM Modem Characterization

Using the modem model shown in Figure 11 of Chapter III, and with an input signal given by Eq (65), the output signal of a DSBAM modem is represented as

$$x(t) = \left[1 + a(t)\right] \cos w_c t$$

$$= (\gamma \cos w_s t + 1) \cos w_c t \qquad (124)$$

58

where $a(t) = \gamma \cos w_s t$ is the input signal. The Fourier transform of Eq (124) is given as (Ref 12:423)

$$X(w) = \frac{\gamma}{4} \delta (w - w_s + w_c) + \frac{\gamma}{4} \delta (w + w_s + w_c)$$

$$+ \frac{\gamma}{4} \delta (w - w_c - w_s) + \frac{\gamma}{4} \delta (w + w_s - w_c)$$

$$+ \frac{\delta}{2} (w - w_c) + \frac{\delta}{2} (w + w_c) \qquad (125)$$

Using Eqs (34) and (125), the power spectral density or more correctly the power spectrum is given as

$$E\{|X_p(w)|^2\} = \frac{\delta}{4} (w - w_c) + \frac{\delta}{4} (w + w_c) + \frac{\gamma^2}{16} \delta (w - w_s + w_c)$$

$$+ \frac{\gamma^2}{16} \delta (w + w_s + w_c) + \frac{\gamma^2}{16} \delta (w - w_c - w_s)$$

$$+ \frac{\gamma^2}{16} \delta (w + w_s - w_c) \qquad (126)$$

where the terms $\delta/4(w - w_c)$ and $\delta/4(w + w_c)$ are delta functions located at the carrier frequencies, w_c and $-w_c$, with each having weight 1/4. The remaining terms are delta functions having weight $\gamma^2/16$, where $0 \le \gamma \le 1$.

DSBAM-SC Modem Characterization

Using the modem model shown in Figure 12 of Chapter III, and with an input signal given by Eq (65), the output signal of a DSBAM-SC modem is represented as

$$x(t) = a(t) \cos w_c t$$

$$= \gamma \cos w_s \cos w_c t \qquad\qquad (127)$$

where $a(t) = \gamma \cos w_s$ is the input signal.

The Fourier transform of Eq (127) is given as (Ref 12: 428)

$$X_p(w) = \frac{\gamma}{4} \delta (w - w_s + w_c) + \frac{\gamma}{4} \delta (w + w_s + w_c)$$

$$+ \frac{\gamma}{4} \delta (w - w_s - w_c) + \frac{\gamma}{4} \delta (w + w_s - w_c) \qquad (128)$$

Since Eq (128) differs from Eq (125) in that the carrier term, $[\delta/2(w - w_c) + \delta/2(w + w_c)]$ has been suppressed, the power spectral density or more correctly the power spectrum is given as

$$E\{|X_p(w)|^2\} = \frac{\gamma^2}{16} [\delta (w - w_c - w_s) + \delta (w + w_c + w_s)$$

$$+ \delta (w - w_c + w_s) + \delta (w + w_c - w_s)] \qquad (129)$$

V. Results and Discussion

This chapter is divided into two sections. The first section covers the characterization results and the second covers the data rate results.

Modem Identification Results

The primary characterization of all modems presented in this study is the power spectral density of the output signal from each modem. Table III lists the modems characterized and the equation for the power spectral density of the output signal from each modem. Comparing the equations in Table III, it can be seen that five of the seven modems listed can be individually identified by the power spectral density. Only the PSK modems (BPSK and QPSK) cannot be distinguished between themselves as the only difference in their power spectral density equations is a constant times the sine squared terms and the width of the signaling interval, T. Neither of these differences can be used to distinguish the BPSK modem from the QPSK modem. Thus, Figure 13 represents a decision tree scheme for identifying the modems listed in Table III using as the decision criteria, the power spectral density.

Since the BPSK and QPSK modems are distinguished only in the general category of PSK modems, a second characterization was chosen to distinguish between individual modems in this general category. The characterization chosen to differentiate the BPSK modem from the QPSK modem was the

TABLE III

Characterization of Modems by Power Spectral Density

| Modem	Power Spectral Density, $E\{|\underline{X}_w|^2\}$ (dBw)
BPSK	$\dfrac{NT^2}{4}\left[\dfrac{\sin^2\left[(w+w_c)T/2\right]}{\left[(w+w_c)T/2\right]^2} + \dfrac{\sin^2\left[(w-w_c)T/2\right]}{\left[(w-w_c)T/2\right]^2}\right]$
QPSK	$2NT^2\left[\dfrac{\sin^2\left[(w+w_c)T\right]}{\left[(w+w_c)T\right]^2} + \dfrac{\sin^2\left[(w-w_c)T\right]}{\left[(w-w_c)T\right]^2}\right]$
BFSK	$\dfrac{NT^2}{8}\left[\dfrac{\sin^2\left[(w\pm w_1)T/2\right]}{\left[(w\pm w_1)T/2\right]^2} + \dfrac{\sin^2\left[(w\pm w_2)T/2\right]}{\left[(w\pm w_2)T/2\right]^2}\right]$
DBFSK	$\dfrac{NT^2}{16}\left[\dfrac{\sin^2\left[(w\pm w_1)t\right]}{\left[(w\pm w_1)T\right]^2} + \dfrac{2\sin^2\left[(w\pm w_2)T\right]}{\left[(w\pm w_2)T\right]^2}\right.$ $\left. + \dfrac{\sin^2\left[(w\pm w_3)T\right]}{\left[(w\pm w_3)T\right]^2}\right]$
BASK	$\dfrac{NT^2}{4}\dfrac{\sin^2\left[(w\pm w_c)T/2\right]}{\left[(w\pm w_c)T/2\right]^2} + \dfrac{1}{4}\left[\delta(w+w_c)\right.$ $\left. + \delta(w-w_c)\right]$
DSBAM	$\dfrac{1}{4}\left[\delta(w+w_c) + \delta(w-w_c)\right] + \dfrac{\gamma^2}{16}\left[\delta(w+w_c+w_s)\right.$ $+ \delta(w-w_c-w_s) + \delta(w-w_c+w_s)$ $\left. + \delta(w+w_c-w_s)\right]$
DSBAM-SC	$\dfrac{\gamma^2}{16}\left[\delta(w-w_c-w_s) + \delta(w+w_c+w_s)\right.$ $\left. + \delta(w-w_c+w_s) + \delta(w+w_c-w_s)\right]$
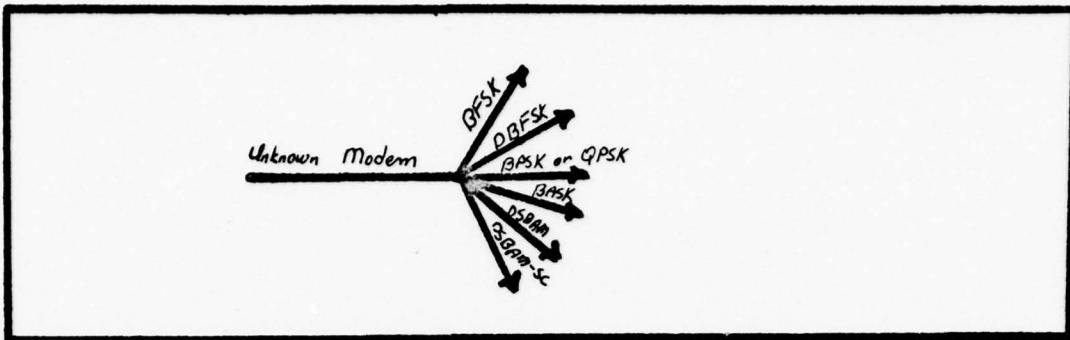
Figure 13.   Modem Identification Decision Tree Scheme
            Using Power Spectral Density as the
            Decision Criteria

autocorrelation function. While the power spectrum and the
correlation form a Fourier transform pair for a wide-sense
stationary process, it is not so for nonstationary processes,
and the processes for BPSK and QPSK are nonstationary.

The autocorrelation functions calculated in Chapter IV
for the BPSK and QPSK modems are listed in Table IV. Com-
parison of these functions shows that the autocorrelation
function can be used to distinguish between a BPSK modem and
a QPSK modem. Figure 14 represents a decision tree scheme
for identifying all the modems listed in Table III. The
term M_i represents the power spectral densities of all the
modems being analyzed. In area H_o of Figure 14, the cri-
teria used to make the decision in identifying a particular
modem is the power spectral density. In the area represented
by H_1, the decision is based on the autocorrelation function.
However, for the autocorrelation function to be a valid means
of identifying the type of modem, the sampling of the output
signal, $x_p(t)$, must occur during the same signaling interval

63

TABLE IV
Characterization of Modems by Autocorrelation Function

| Modem	Autocorrelation Function, $R(t_1, t_2)$
BPSK	$\begin{cases} 0 & \text{when } t_1 \text{ and } t_2 \text{ are not in the same signaling interval} \\ \cos w_c t_1 \cos w_c t_2 & \text{when } t_1 \text{ and } t_2 \text{ are in the same signaling interval} \end{cases}$
QPSK	$\begin{cases} 0 & \text{when } t_1 \text{ and } t_2 \text{ are not in the same signaling interval} \\ \sin w_c t_1 \sin w_c t_2 \\ + \cos w_c t_1 \cos w_c t_2 & \text{when } t_1 \text{ and } t_2 \text{ are in the same signaling interval} \end{cases}$

Figure 14. Modem Identification Decision Tree Scheme Using Power Spectral Density and the Auto-correlation Function as the Decision Criteria

for times t_1 and t_2. A correlator and frequency spectrum analyzer can be used to determine the autocorrelation function and power spectral density, respectively.

Data Rate Identification Results

The equations for the power spectral densities of the modems listed in Table III (except for the DSBAM and DSBAM-SC modems), were used to construct power spectral density curves for various data rates. In the equations listed in Table III (except for the QPSK modem), the data rate is represented as T^{-1}, where T is the signaling interval. In the equation for the QPSK modem, T^{-1} represents symbol rate and T is the signaling interval. The power spectral curves (only the positive half) generated are presented in Appendix A, Figures 15 through 31, along with a list of the data rates and carrier frequencies used in constructing the curves. The data rates, given in bits per second (BPS), and the carrier frequencies, given in hertz (Hz), are valid modem specifications.

The power spectral density curves in Appendix A were used to determine the data rate (symbol rate for the QPSK modem) of the output signal, $x_p(t)$, primarily by using two different methods.

The first method involved measuring the width of the main lobe (lobe with the largest amplitude) at the crossover points on the frequency axis and dividing this value by two. For the QPSK modem, this method gives the symbol rate. For

the BFSK modem, Figures 23, 24, and 25, only one of the
main lobes was used, and for Figure 26, the entire curve
was assumed to be the main lobe.

The second method involved measuring the width of the
main lobe at the 3 dB points. For the BFSK modem, Figures
23, 24, and 25, only one of the main lobes was used, and
for Figure 26, the entire curve was assumed to be the main
lobe.

The analytical results of these two methods are listed
in Table V. Using the main lobe crossover method proved to
be a valid method for determining the data rate except for
the BFSK modem at 1200 BPS and the DBFSK modem at 2400 BPS.
The analytical results of the 3 dB point method, Table V,
were not as valid as the results for the main lobe cross-
over method, especially for the BFSK modem at 1200 BPS.

A secondary or third method was tried to more accu-
rately determine the data rate of the BFSK modem at 1200
BPS. The assumption used in the first two methods, that
the power spectral density curve for the FBSK modem at 1200
BPS, Figure 26, was one single main lobe, was changed. The
curve in Figure 26 was now assumed to be composed of two
main lobes which if Figures 23, 24, and 25 are viewed, sup-
ports this assumption. As the data rate is increased, the
main lobes get closer together until they overlap or merge
as is shown in Figure 26 when the data rate is 1200 BPS.
Thus, the third method was based on measuring the width
between the two peaks of curve shown in Figure 26. As a

66

TABLE V

Predicted Versus Actual Modem Data Rate Values

Modem	Data Rate (BPS)*		
	Actual	3 dB Point Method	Main Lobe Crossover Method
BPSK	150	120	150
	300	270	300
	600	540	600
	1200	1060	1200
QPSK*	150	120	150
	300	270	300
	600	540	600
	1200	1060	1200
BFSK	150	120	150
	300	280	300
	600	580	600
	1200	2280	1470
DBFSK	2400	1530	1500
BASK	150	120	150
	300	270	300
	600	540	600
	1200	1060	1200
* For the QPSK modem, the rates listed are symbol rates expressed as symbols per second (SPS).			

result, this method produced a data rate of 1200 BPS as compared to the actual data rate of 1200 BPS.

A fourth method was tried to more accurately determine the data rate of the DBFSK modem at 2400 BPS. From the discussion on the DBFSK modem in Chapter III and from (Ref 11: 128), the major advantage of duobinary encoding is the pseudo-compression of the spectrum along the frequency axis when the input binary signal is in the form of a rectangular pulse train. This means that certain parameters in the spectrum, which are sometimes used to define bandwidth in a loose sense, are also halved. One of these is the frequency at which the spectrum goes to zero or the first crossover point of the spectrum on the frequency axis. In essence, duobinary encoding allows for higher data rates to be transmitted in the same bandwidth (in loose terms) as lower data rates of binary signals. The binary signal is restricted in this case to a rectangular pulse train. Therefore, the original method used to obtain the result in the main lobe crossover method (Table V) was changed in that only the width of the main lobe at the crossover points on the frequency axis is used as the measure of the data rate. As a result, this method produced a data rate of 3000 PBS as compared to the actual data rate of 2400 BPS.

Of the methods used to determine the data rate (symbol rate for QPSK modem), only the main lobe crossover method was successful except for determining the data rates for the BFSK modem at 1200 BPS and the DBFSK modem at 2400 BPS.

68

This method is not a valid predictor of the data rate for these modems at the data rate specified because of the uncertainty of the width of the main lobes due to the merger of the two lobes in the power spectral curve for the BFSK modem and of the merger of the three lobes in the power spectral curve for the DBFSK modem. An alternate method was used to determine the data rate of the BFSK modem when the two main lobes merged and although it proved successful, it is considered valid only in the case used. The alternate method used to determine the data rate of the DBFSK modem proved unsuccessful.

VI. Conclusions and Recommendations

Conclusions

The major conclusion reached in this study is that
modems can be characterized by the real time measurement of
the power spectral density and the autocorrelation function
of the output signal from the modem. This characterization
in turn leads to the identification of the modulation scheme
being used as each modem or group of modems has a unique
power spectral density. To identify individual modems with-
in a group, the autocorrelation function can be used.

Another conclusion is that, in most instances, the data
rate (symbol rate for QPSK modem) can be determined by ob-
serving the width of the main lobes of the power spectral
curves. However, this is valid only when the main lobes do
not merge as in the BFSK and DBFSK modems.

Recommendations

The power spectral density curves presented in Appendix
A could be used as templates or as overlays to be placed on
spectrum analyzers in order that an operator might determine
the modulation scheme of the modem. Additionally, the ope-
rator could determine the data rate (symbol rate for QPSK
modem) at which the modem is operating by measuring half
the width of the main lobe at the crossover points on the
frequency axis of the power spectral density curve. How-
ever, this is a valid test only when main lobes do not merge

70

as in the case for the BPSK modem at 1200 BPS and the DBFSK modem at 2400 BPS.

As a result of the conclusions and the research required for this study, the following recommendations are submitted for future studies in this area.

1. Since this study presents only theoretical results on the characterization of modems by the power spectral density and the autocorrelation functions, empirical data is needed to test the conclusions. Additionally, the study should include how additive interference (i.e., additive white gaussian noise) and other multiplicative effects such as fading (a time-varying channel attenuation and phase shifting of the desired wave) affect the characterization of modems using second moment characterizations.

2. Additional research is needed to find a method for determining the data rate at which a modem is operating.

3. A future study would be to investigate the possibility of using some feature or parameter, once a modem has been identified, to do degradation analysis on the received signal in a technical control facility. Developing such a method could possibly aid in assessing the performance of communications links and enable action to be taken before serious degradation occurs.

71

4.   Research should be conducted in automating the
     identification of modem type and data rate.

One approach in automating the identification of modem
type would be to use a Fast Fourier Transform (FFT) algo-
rithm to transform the modem's output signal (or received
signal from the channel) from the time-domain to the fre-
quency-domain and calculate the power spectral density. An
algorithm would then be used to compare the calculated power
spectral density with other known power spectral densities
as a means of identifying the type of modem. It should be
noted that the power spectrum and the correlation form a
Fourier transform pair for a wide-sense stationary process,
but not for nonstationary processes. Therefore, taking the
inverse FFT of the power spectral density will not result
in finding the complete autocorrelation function if the
process is nonstationary.

Bibliography

1. Angell, S. K. <u>Modem Recognition Algorithms Feasibility Report</u>. Scott Air Force Base, Illinois: Air Force Communications Service/Office of Operations Analysis, December 1977.

2. Bennett, W. R. <u>Introduction to Signal Transmission</u>. New York: McGraw-Hill Book Company, 1970.

3. Bennett, W. R. "Statistics of Regenerative Digital Transmission," <u>Bell Systems</u> Technical Journal, <u>37</u>: 1501-1542 (November 1958).

4. Bracewell, R. N. <u>The Fourier Transform and Its Applications</u>. New York: McGraw-Hill Book Company, 1965.

5. "Duobinary Coding," Selected Articles from the Lenkurt Demodulator, <u>Volume 1</u>: 399-404. GTE Lenkurt Incorporated, 1971.

6. Lee, Y. W., T. P. Cheatham, Jr., and J. B. Wiesner. "Application of Correlation Analysis to the Detection of Periodic Signals in Noise," <u>Proc IRE</u>, <u>38</u>: 1165-1171 (October 1950).

7. Lee, Y. W. <u>Statistical Theory of Communications</u>. New York: John Wiley and Sons, 1960.

8. Lender, A. "The Duobinary Technique for High-Speed Data Transmissions," <u>IEEE Transactions on Communications and Electronics</u>, 82-83, No 66: 214-218 (May 1963).

9. Lucky, R. W., J. Solz, and E. J. Wildon, Jr. <u>Principles of Data Communications</u>. New York: McGraw-Hill Book Company, 1968.

10. Papoulis, A. <u>Probability, Random Variables and Stachostic Processes</u>. New York: McGraw-Hill Book Company, 1965.

11. Sekey, A. "An Analysis of the Duobinary Technique," <u>IEEE Transactions on Communications Technology</u>, COM-14, No 2: 126-130 (April 1966).

12. Thomas, J. B. <u>An Introduction to Statistical Communications Theory</u>. New York: John Wiley and Sons, 1969.

13. Ziemer, R. E., and W. H. Tranter. <u>Principles of Communications</u>. Boston: Houghton Mifflin Company, 1976.

Appendix A

Power Spectral Density Curves

This appendix contains the power spectral density curves (only the positive half) for the modems listed in Table III. The power spectral density equations (positive half only) in Table III were used to construct the curves for different values of T, the signaling interval. The inverse of T is called the data rate (except for the QPSK modem, it is called the symbol rate) and the values of T^{-1} and the carrier frequencies used in the equations of Table III are listed in Table VI of this appendix. The data rates are in bits per second (BPS) (except for the QPSK modem, the rate is in symbols per second (SPS)) and the carrier frequencies are given in hertz (Hz).

TABLE VI

Carrier Frequencies and Data Rates Used to Construct Power Spectral Density Curves

Modem	Carrier Frequency (Hz)	Data Rate (BPS)[*]
BPSK	$w_c = 1800$	150,300,600,1200
QPSK[*]	$w_c = 1800$	150,300,600,1200
BFSK	$w_1 = 1200$	150,300,600,1200
	$w_2 = 2400$	
DBFSK	$w_1 = 1200$	2400
	$w_2 = 1800$	
	$w_3 = 2400$	
BASK	$w_c = 1800$	150,300,600,1200

[*] Rate for the QPSK modem is a symbol rate instead of a data rate.
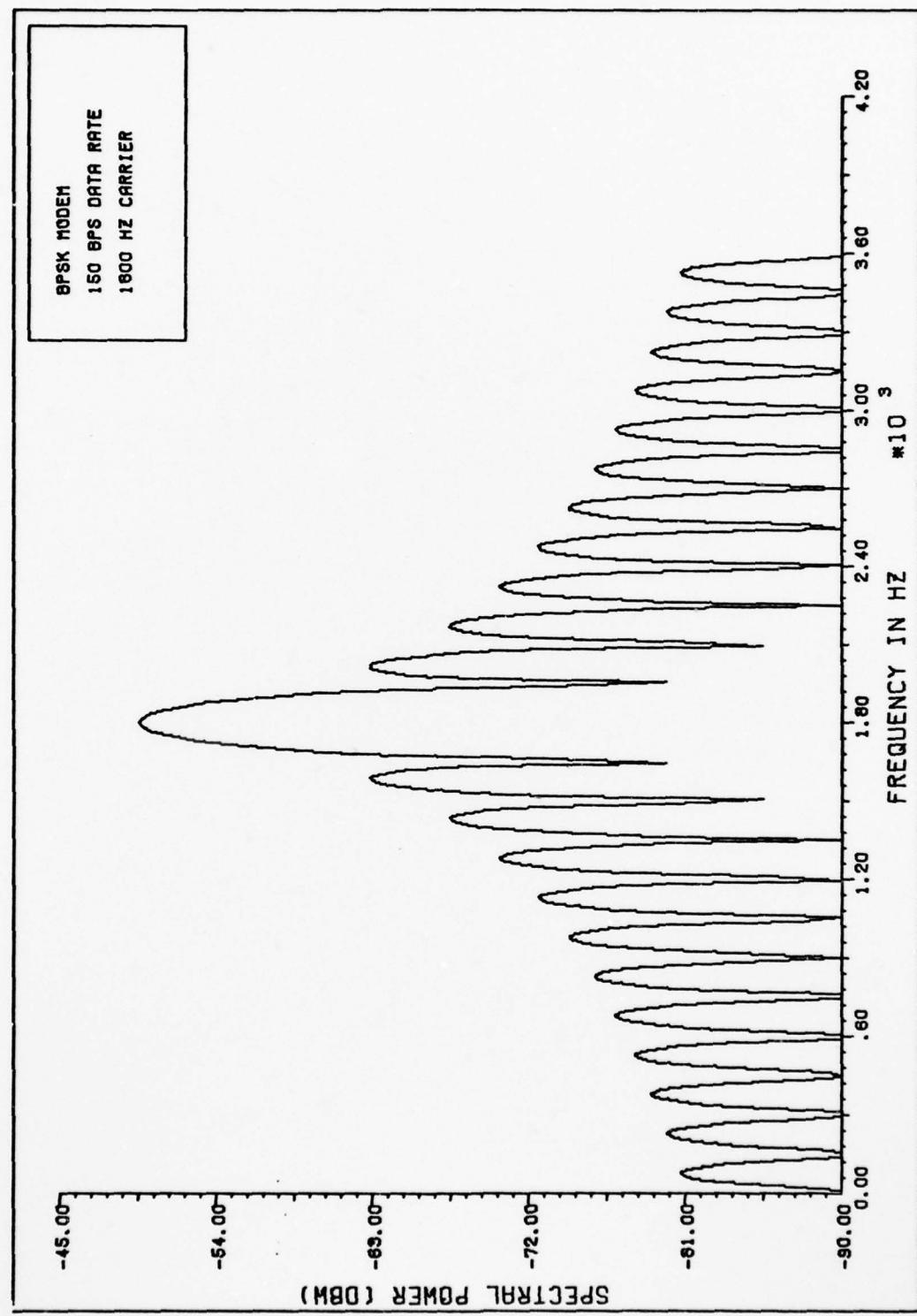
Figure 15. Power Spectral Density Curve for BPSK Modem With Data Rate, 150 BPS
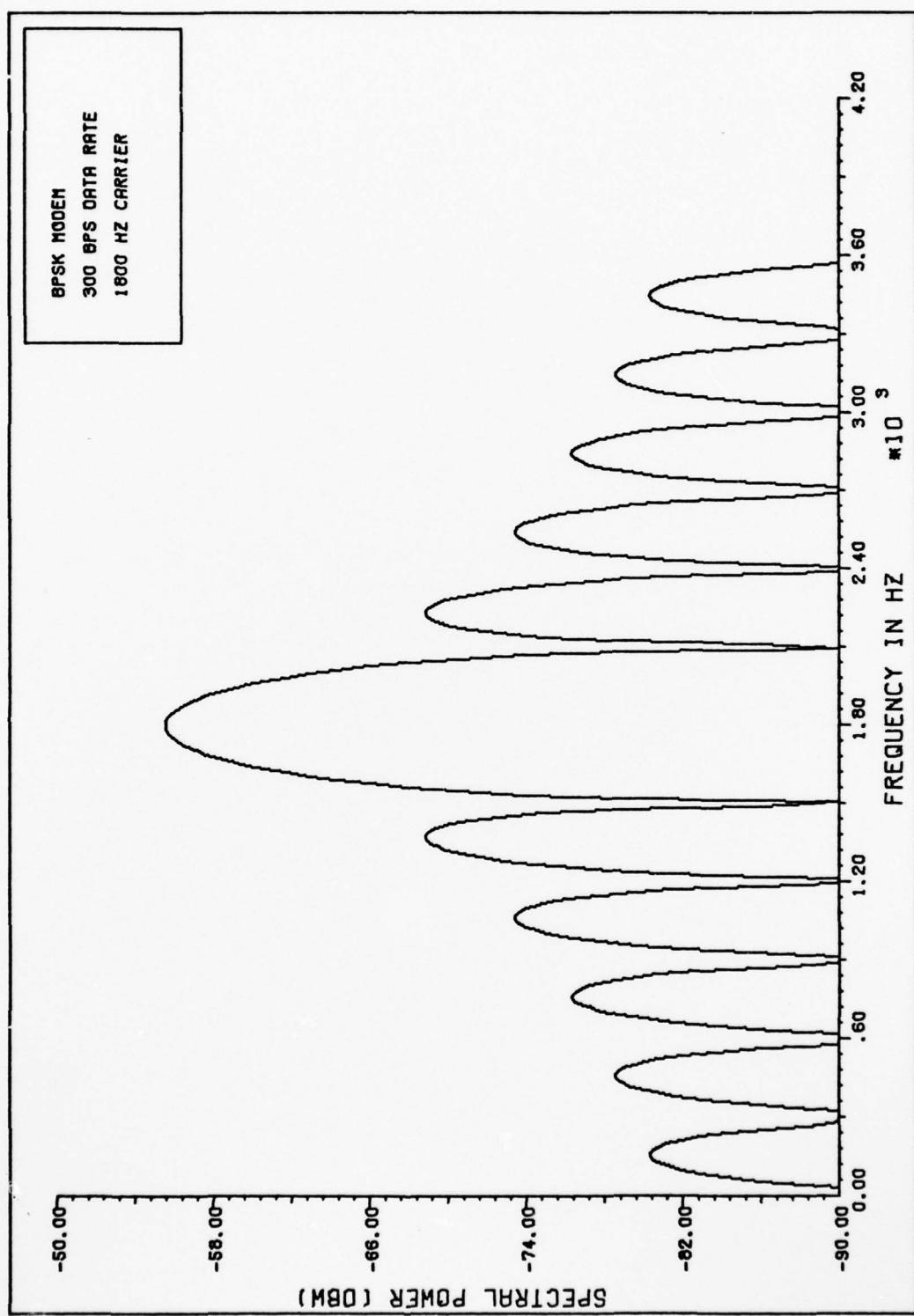
Figure 16. Power Spectral Density Curve for BPSK Modem With Data Rate, 300 BPS
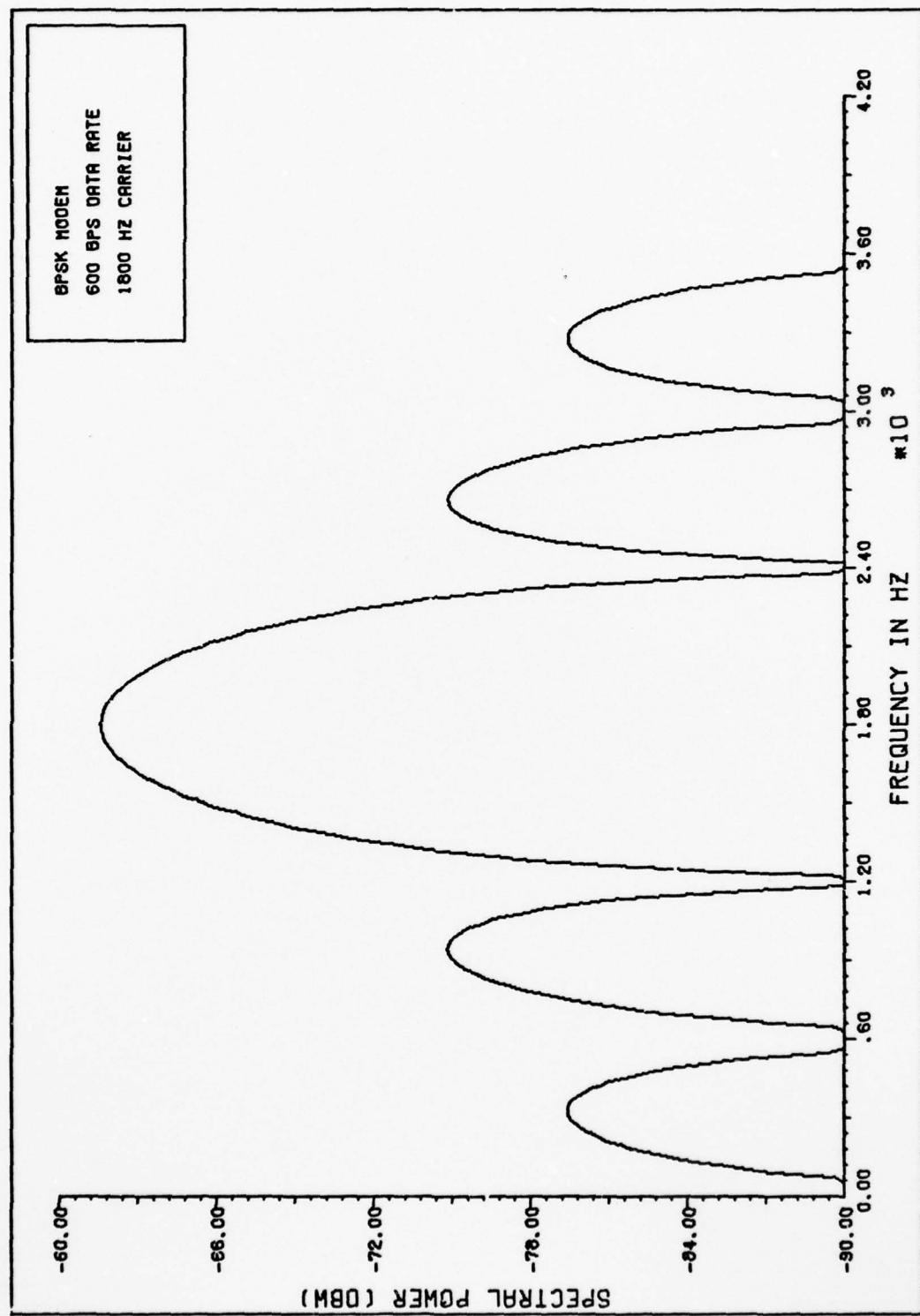
Figure 17. Power Spectral Density Curve for BPSK Modem With Data Rate, 600 BPS

78
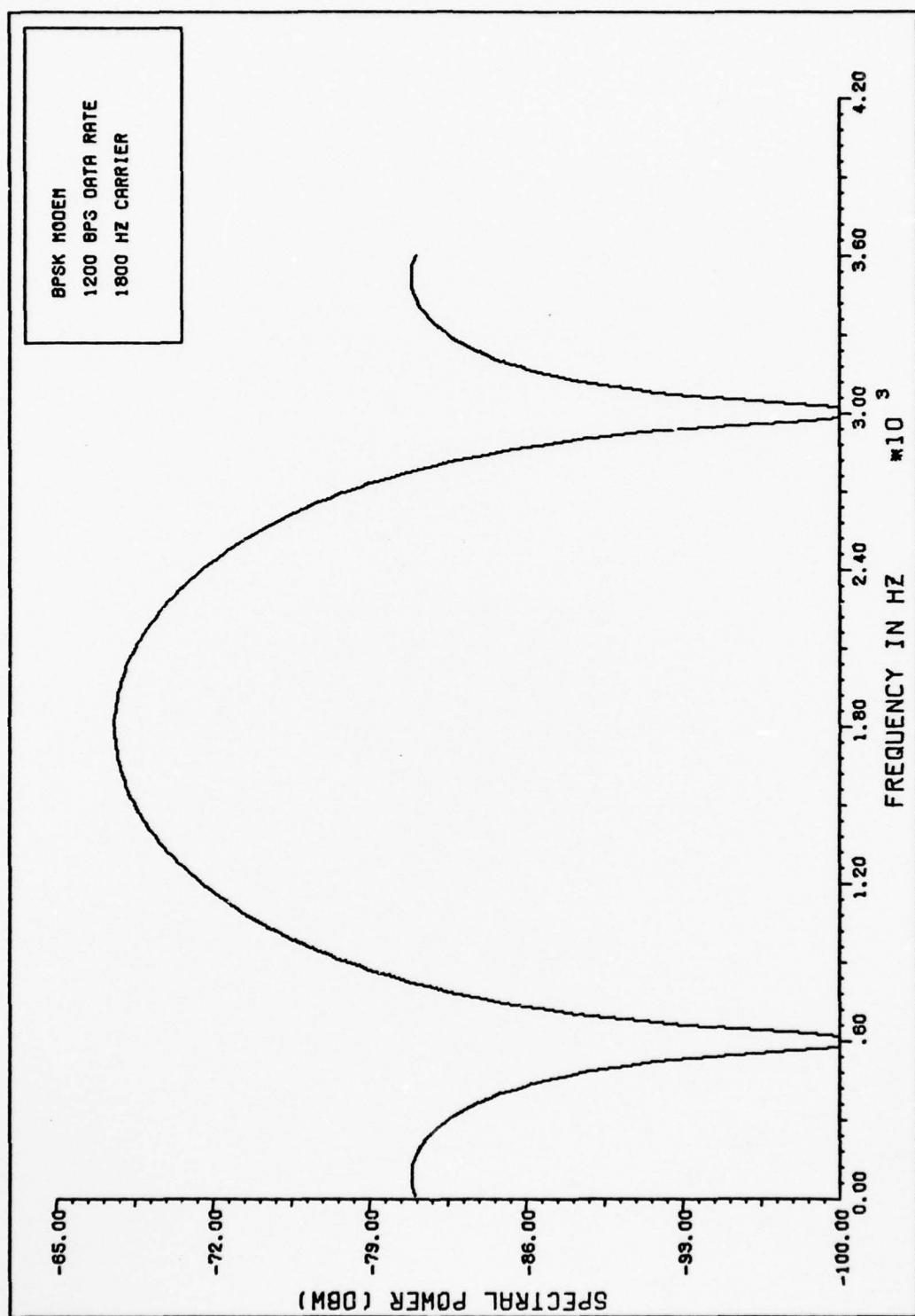
Figure 18. Power Spectral Density Curve for BPSK Modem With Data Rate, 1200 BPS
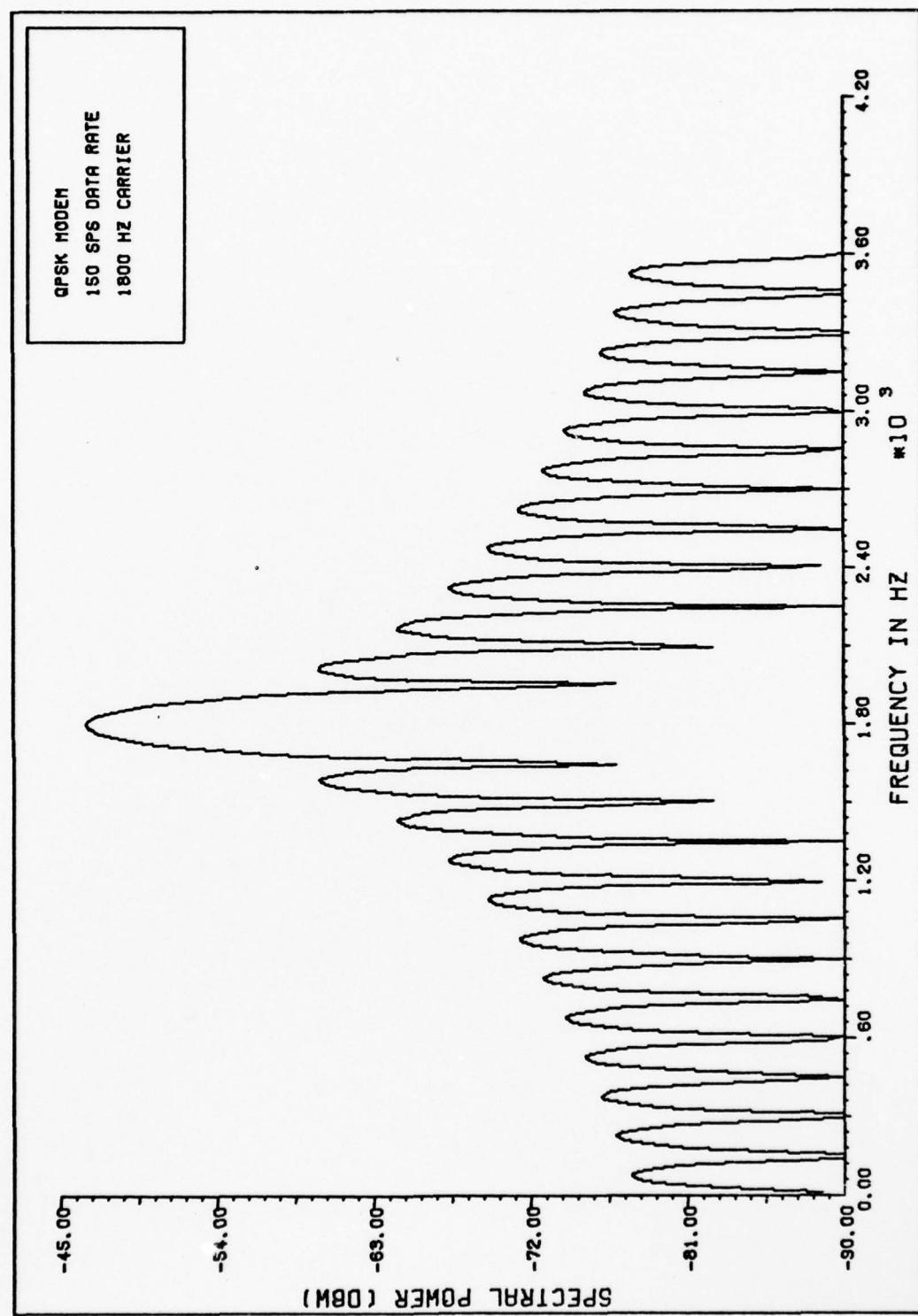
Figure 19. Power Spectral Density Curve for QPSK Modem With Symbol Rate, 150 SPS

80
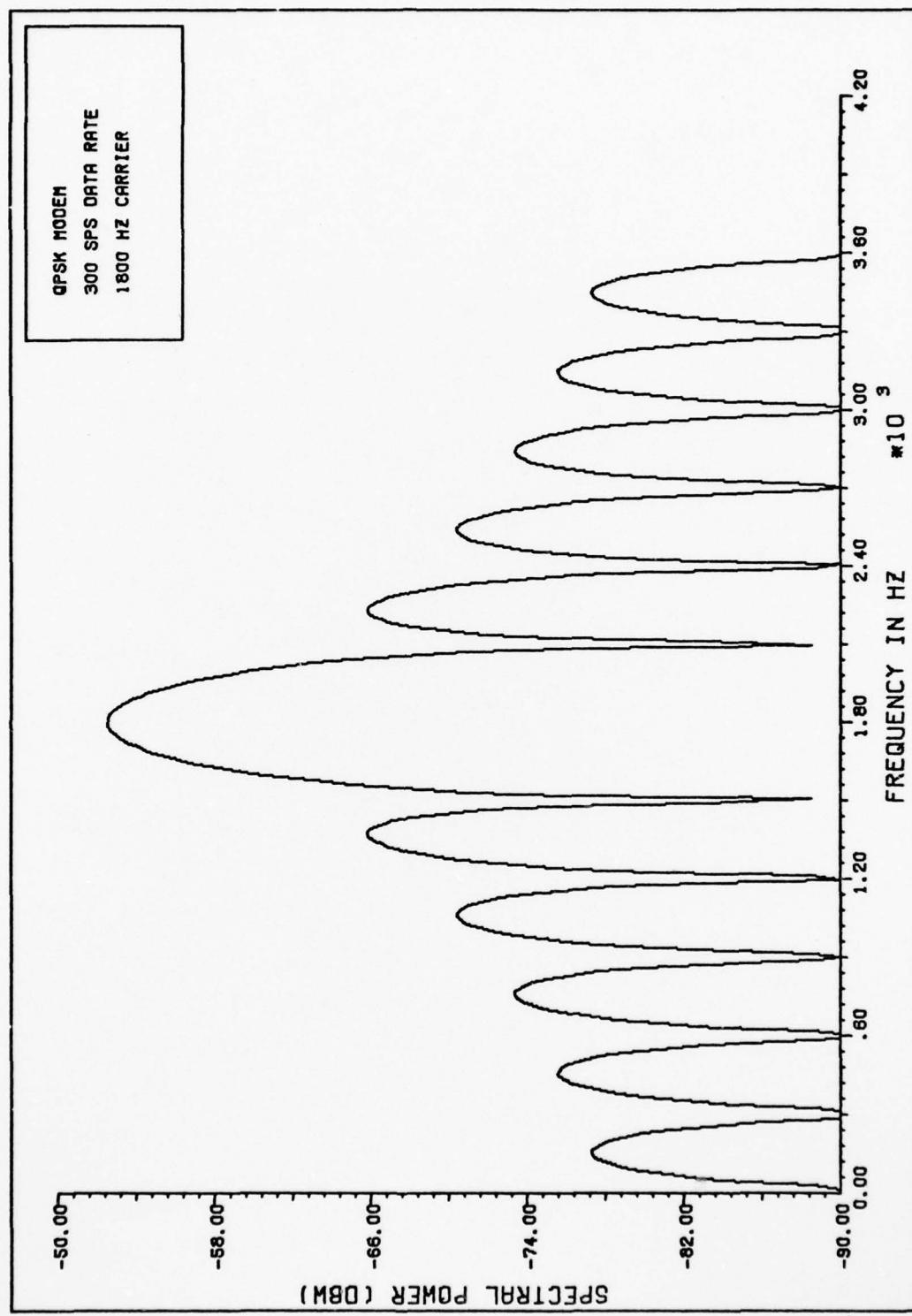
Figure 20. Power Spectral Density Curve for QPSK Modem With Symbol Rate, 300 SPS

81
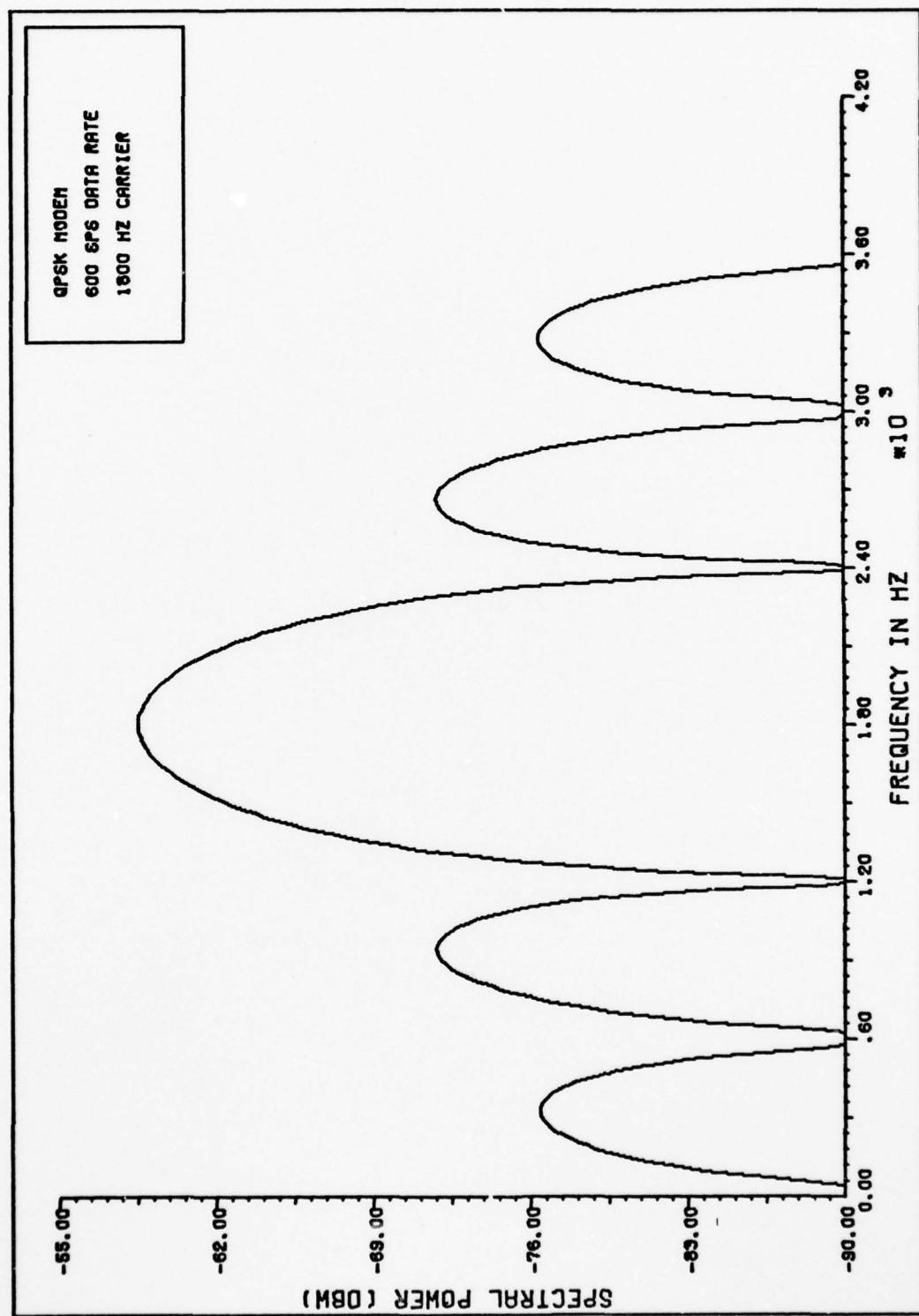
Figure 21. Power Spectral Density Curve for QPSK Modem With Symbol Rate, 600 SPS
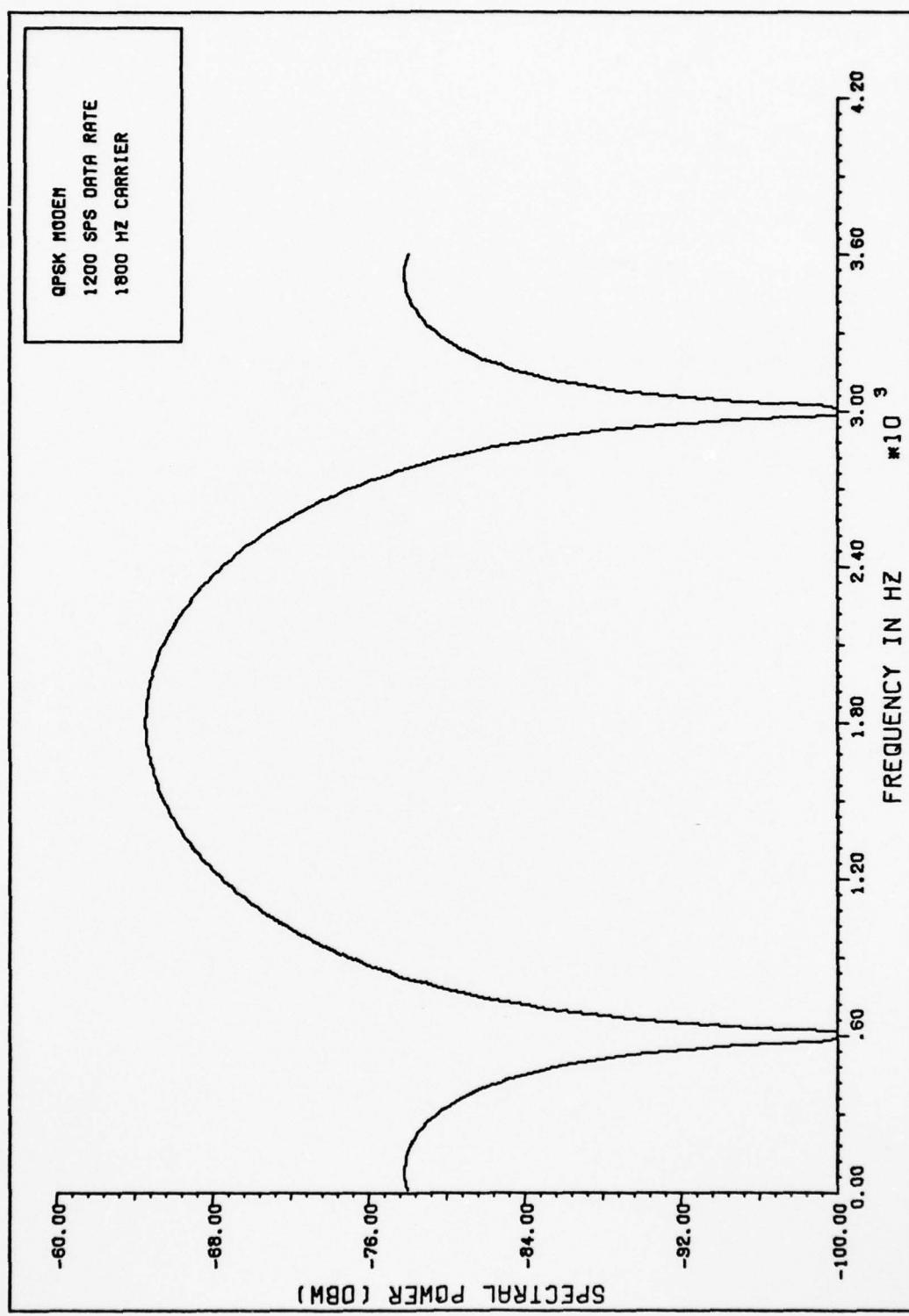
Figure 22. Power Spectral Density Curve for QPSK Modem With Symbol Rate, 1200 SPS

83
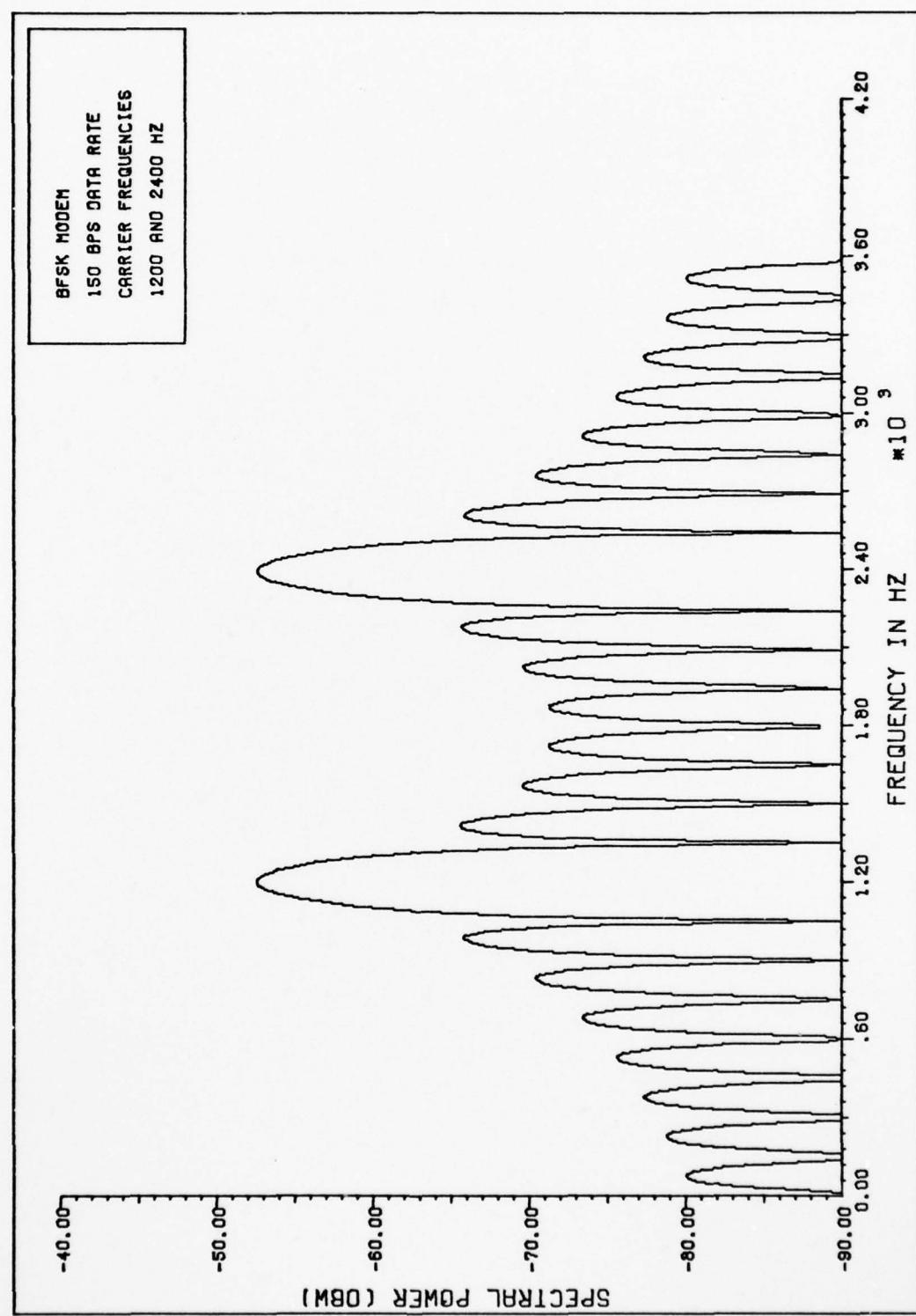
Figure 23. Power Spectral Density Curve for BFSK Modem With Data Rate, 150 BPS

84
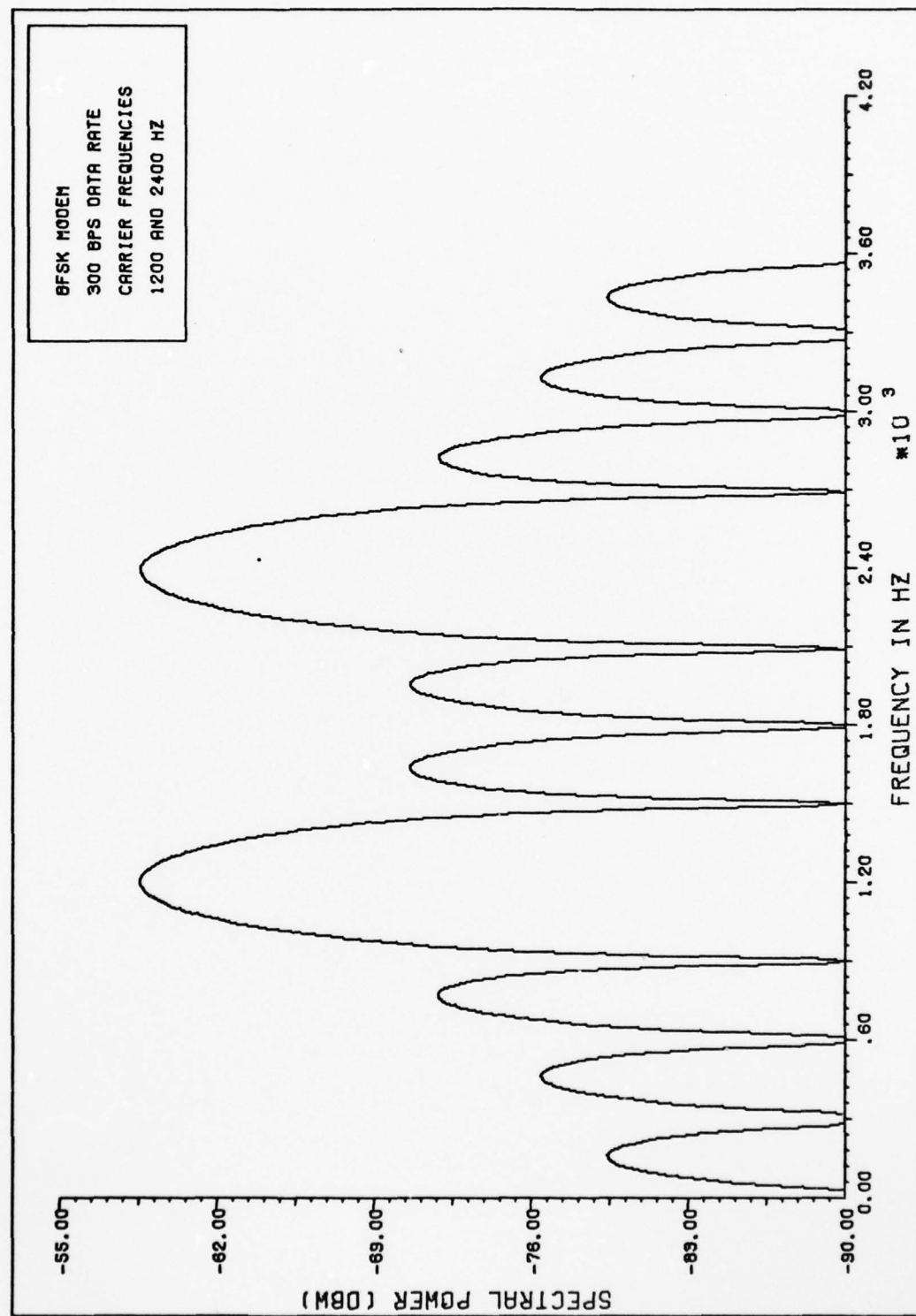
Figure 24. Power Spectral Density Curve for BFSK Modem With Data Rate, 300 BPS

85
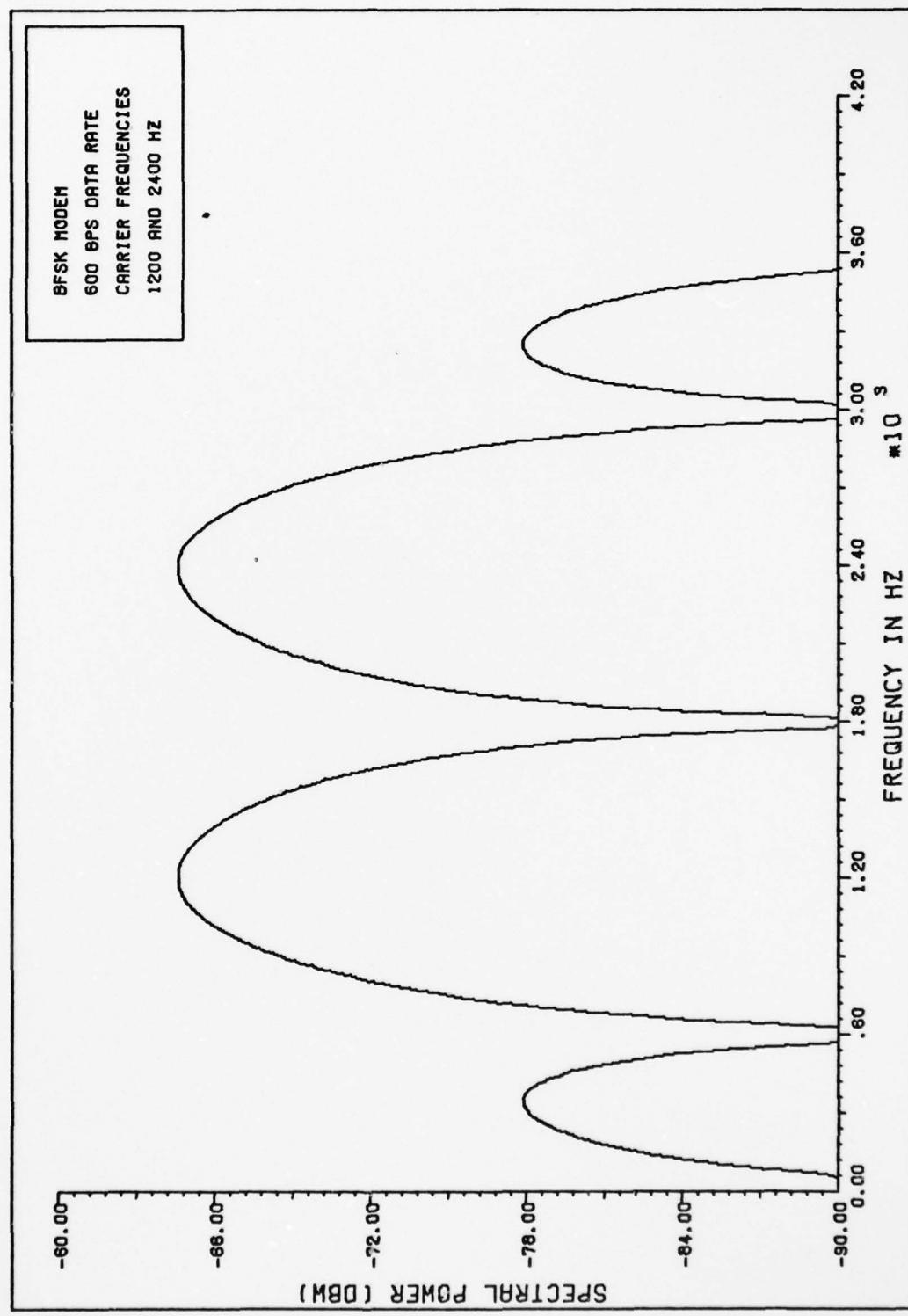
Figure 25. Power Spectral Density Curve for BFSK Modem With Data Rate, 600 BPS

86

MICROCOPY RESOLUTION TEST CHART

NATIONAL BUREAU OF STANDARDS-1963-A
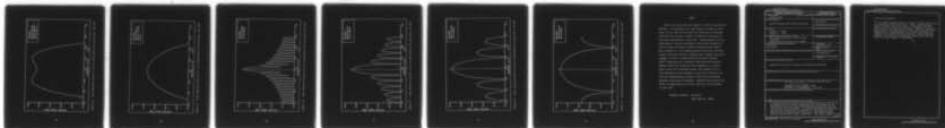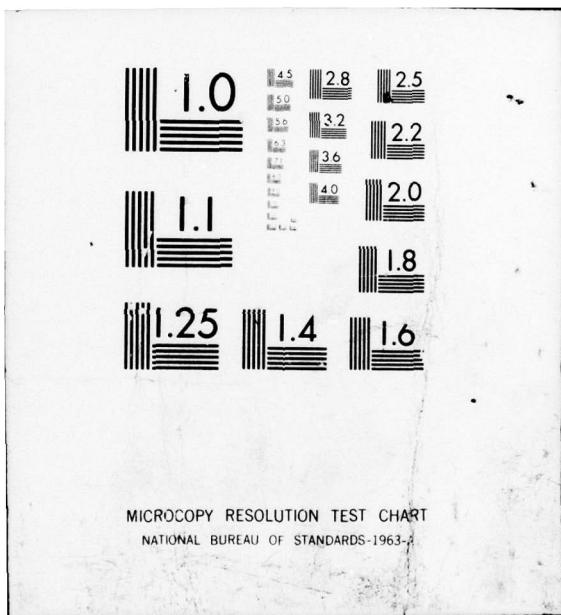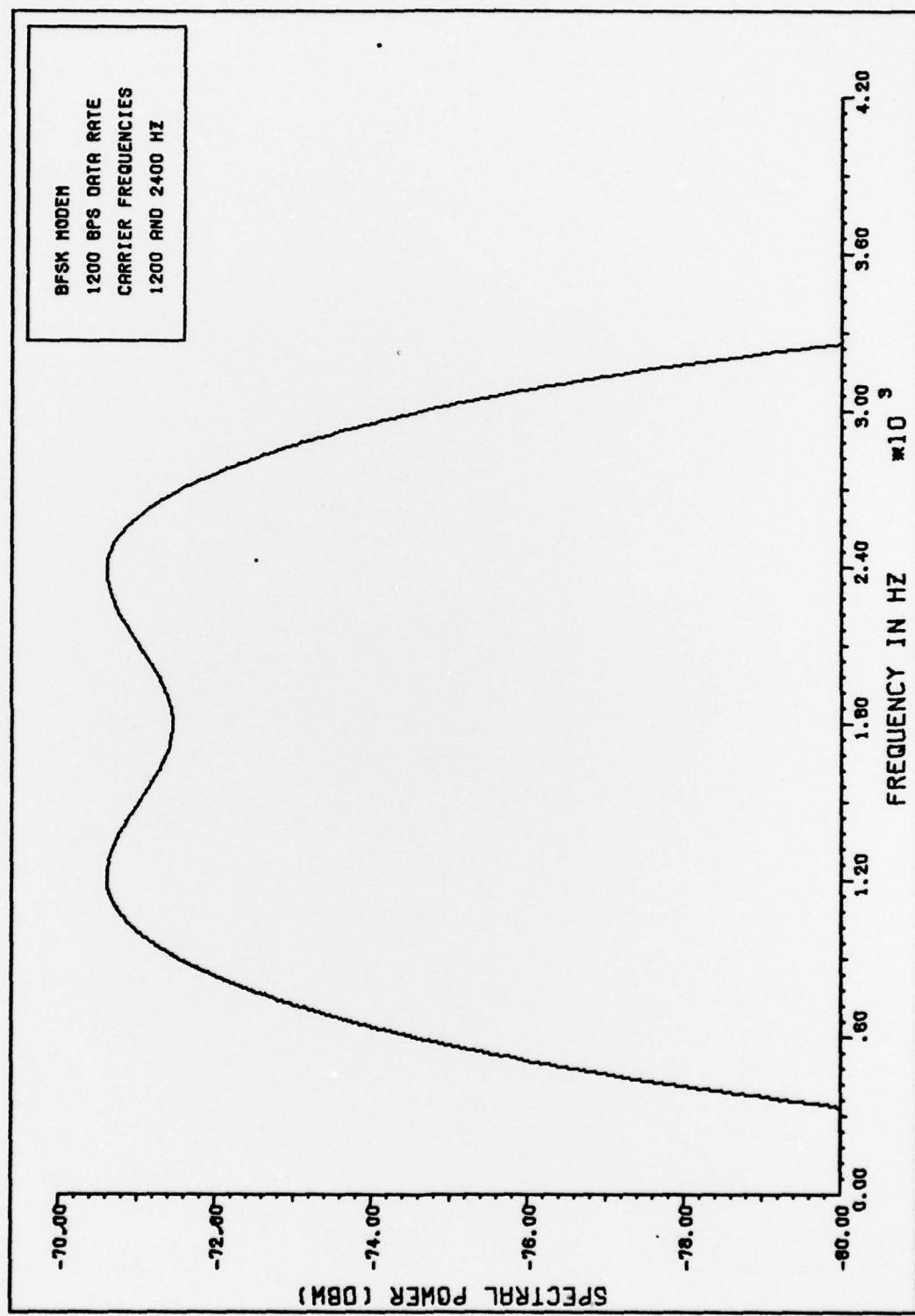
Figure 26. Power Spectral Density Curve for BFSK Modem With Data Rate, 1200 BPS
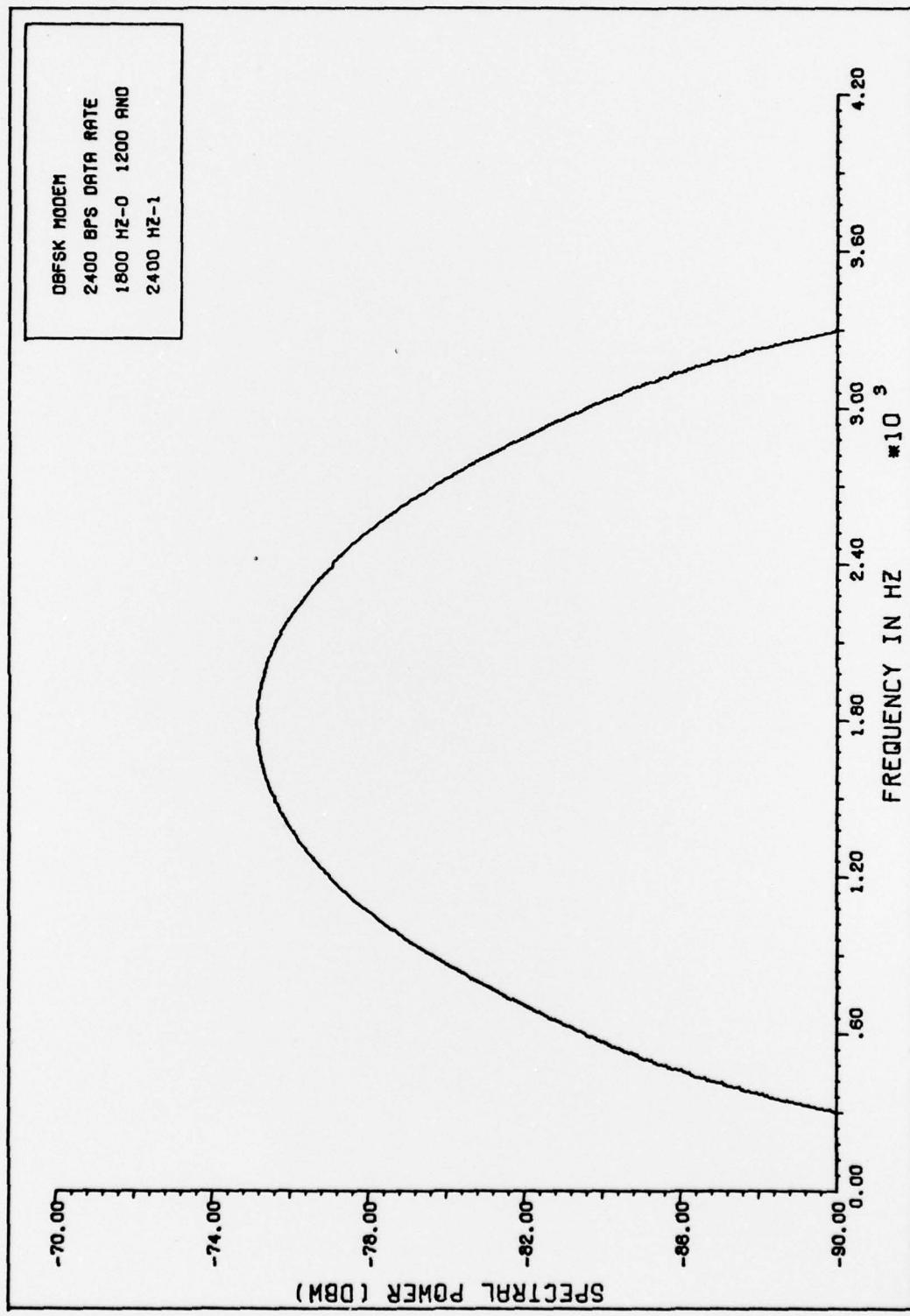
Figure 27. Power Spectral Density Curve for DBFSK Modem With Data Rate, 2400 BPS
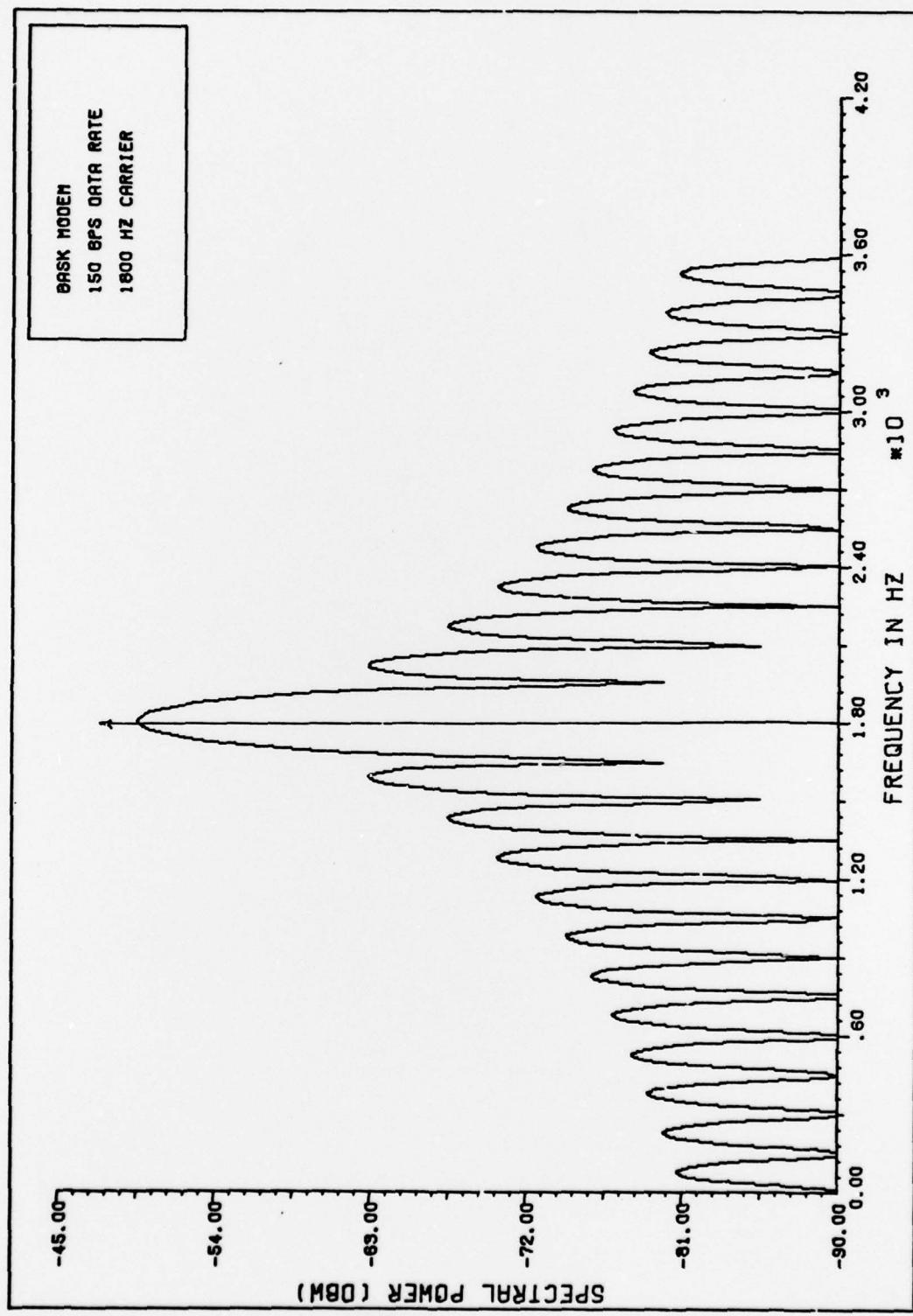
Figure 28. Power Spectral Density Curve for BASK Modem With Data Rate, 150 BPS
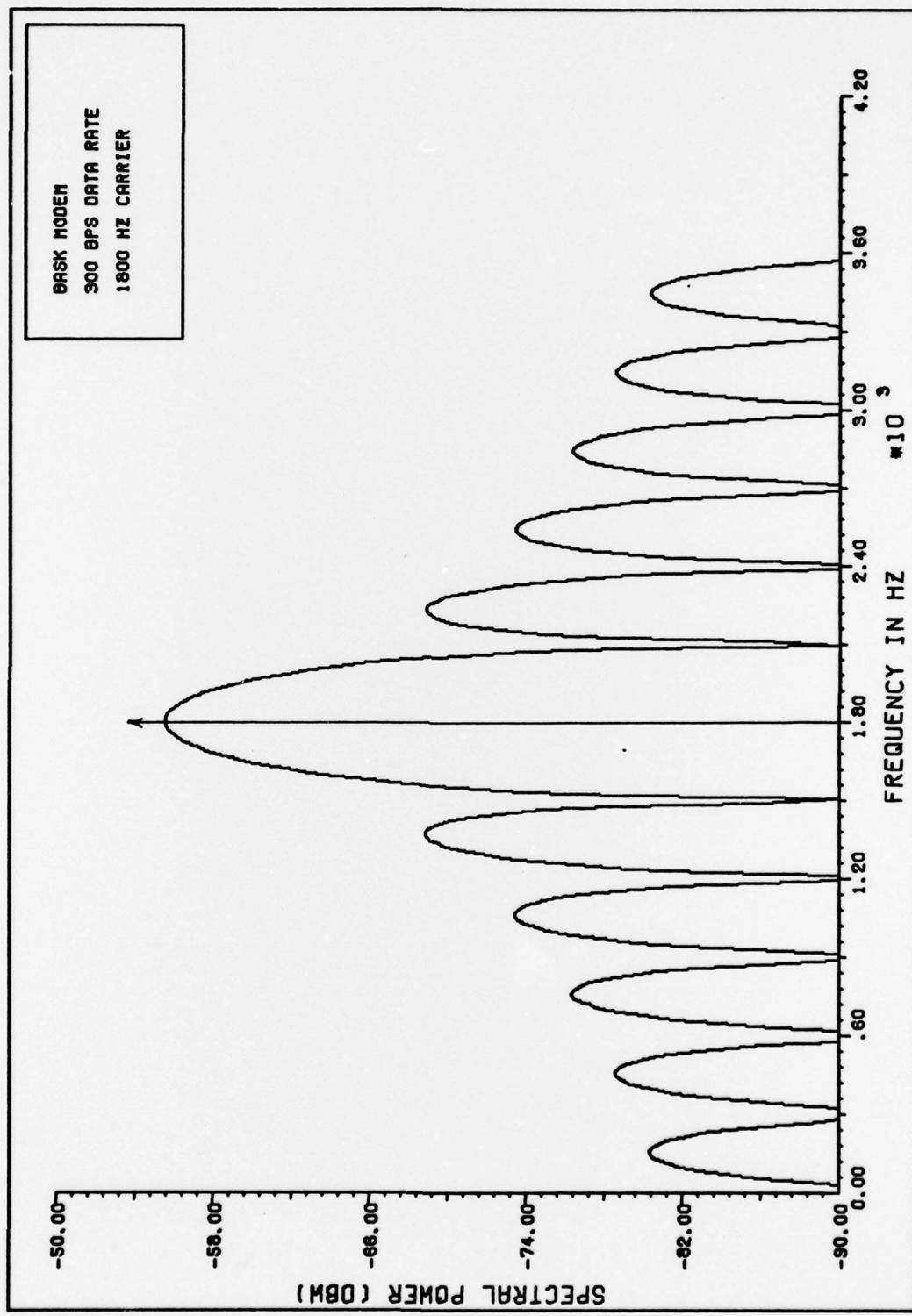
Figure 29. Power Spectral Density Curve for BASK Modem With Data Rate, 300 BPS
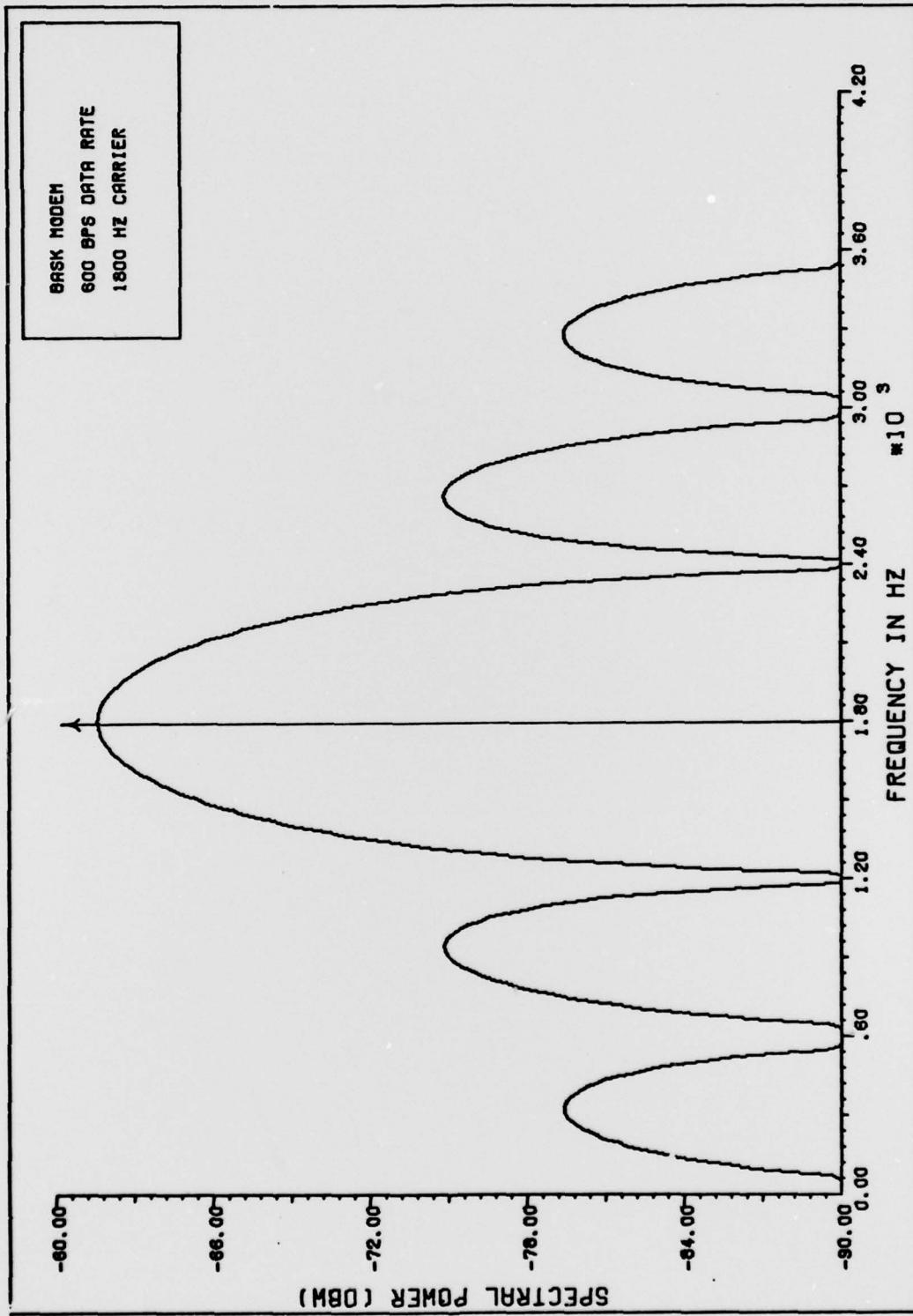
Figure 30. Power Spectral Density Curve for BASK Modem With Data Rate, 600 BPS

91
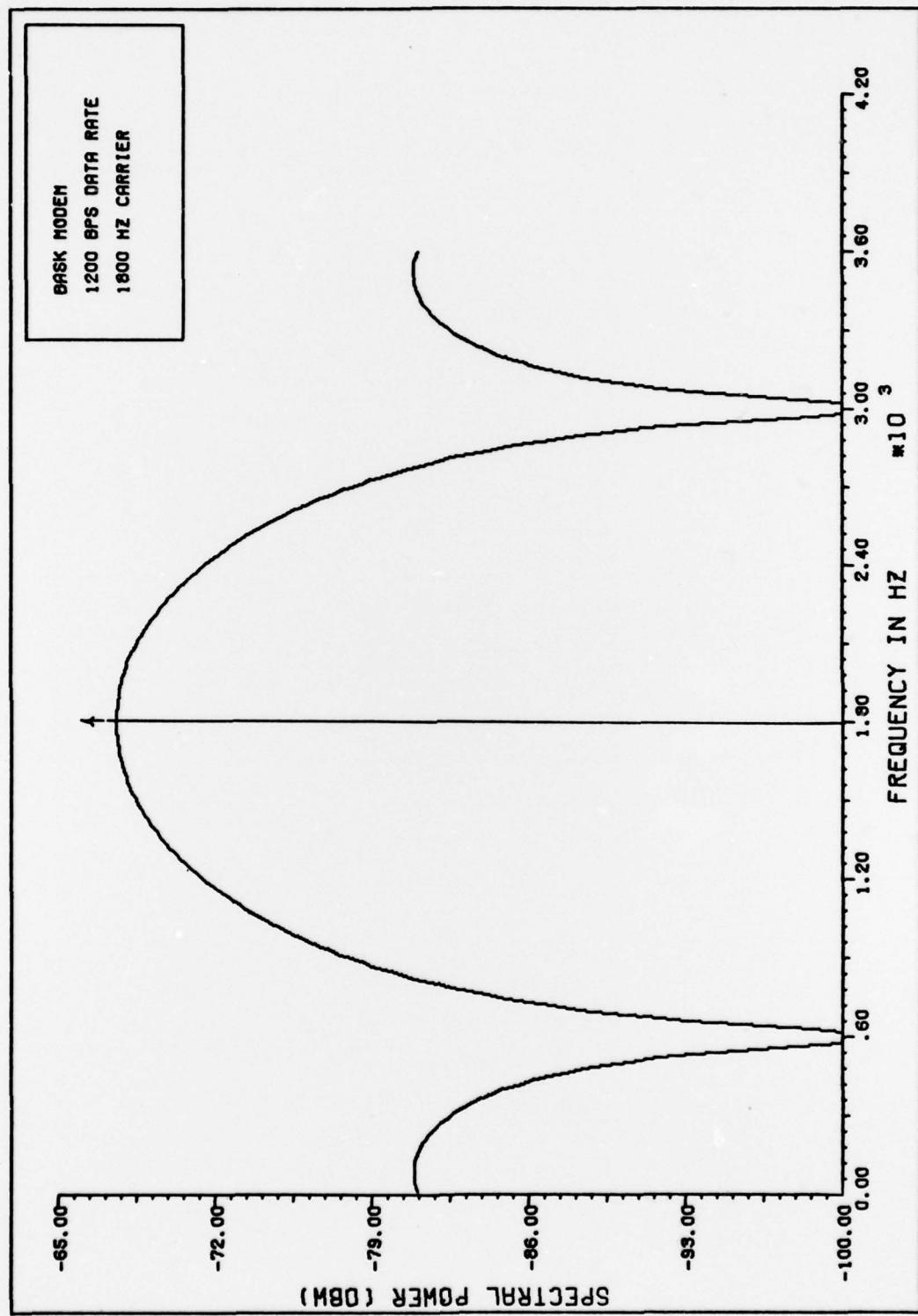
Figure 31. Power Spectral Density Curve for BASK Modem With Data Rate, 1200 BPS

<u>Vita</u>

Robert Leo Jones was born August 19, 1947 in Louisville, Kentucky. He graduated from high school in Flaherty, Kentucky in June 1965 and attended the University of Kentucky from which he received a degree of Bachelor of Science in Electrical Engineering in May 1970. Upon graduation he was commissioned a Second Lieutenant in the United States Air Force through the Reserve Officers Training Corps (ROTC). Upon completion of the Communications-Electronics Officers course at Keesler AFB MS in January 1971, Captain Jones was assigned as Chief, Communications-Electronics Branch, 2020th Communications, Squadron, Shaw AFB South Carolina. Captain Jones then served as Site Commander of a remote radio relay site in Eastern Turkey from January 1974 to 1975 whereupon he was assigned as the Chief, Tactical Control and Landing Systems Branch, 1868 Facility Checking Squadron, Rhein Main AB Germany. Captain Jones entered the School of Engineering, Air Force Institute of Technology in June 1977.

　　　　　　　Permanent address:　305 Floyd
　　　　　　　　　　　　　　　　　Lynn Haven FL　32444

REPORT DOCUMENTATION PAGE		READ INSTRUCTIONS BEFORE COMPLETING FORM
1. REPORT NUMBER GE/EE/78-30	2. GOVT ACCESSION NO.	3. RECIPIENT'S CATALOG NUMBER
4. TITLE (and Subtitle) Modem Modeling and Characterization		5. TYPE OF REPORT & PERIOD COVERED MS Thesis
		6. PERFORMING ORG. REPORT NUMBER
7. AUTHOR(s) Robert L. Jones Captain USAF		8. CONTRACT OR GRANT NUMBER(s)
9. PERFORMING ORGANIZATION NAME AND ADDRESS Air Force Institute of Technology (AFIT/EN) Wright-Patterson AFB, Ohio 45433		10. PROGRAM ELEMENT, PROJECT, TASK AREA & WORK UNIT NUMBERS
11. CONTROLLING OFFICE NAME AND ADDRESS HQ AFCS/OA Scott AFB IL		12. REPORT DATE December 1978
		13. NUMBER OF PAGES 102
14. MONITORING AGENCY NAME & ADDRESS(if different from Controlling Office)		15. SECURITY CLASS. (of this report) Unclassified
		15a. DECLASSIFICATION/DOWNGRADING SCHEDULE

16. DISTRIBUTION STATEMENT (of this Report)

Approved for public release; distribution unlimited.

17. DISTRIBUTION STATEMENT (of the abstract entered in Block 20, if different from Report)

18. SUPPLEMENTARY NOTES   Approved for public release; IAW AFR 190-17

JOSEPH P. HIPPS, Major, USAF
Director of Information   1-19-79

19. KEY WORDS (Continue on reverse side if necessary and identify by block number)

20. ABSTRACT (Continue on reverse side if necessary and identify by block number)
A method for modem modeling and characterization is presented.
The properties of Fourier transforms and the properties of
correlation and power spectral density for periodic and ran-
dom functions are reviewed. The modems modeled are character-
ized by the theoretical calculation of the power spectral
density and autocorrelation function of the output signal
from the modem under ideal conditions. The input signal→next
page

DD FORM 1473   EDITION OF 1 NOV 65 IS OBSOLETE
1 JAN 73

Block 20 Continued:

to the modems characterized is either a random pulse train or a special periodic function. Also, power spectral density curves are constructed to determine the data rate at which a modem is operating. Though no empirical data exists, the theoretical calculations indicate that modems can be characterized by the power spectral density and the autocorrelation function. More research, however, is needed for accurately determining the data rate at which a modem is operating.